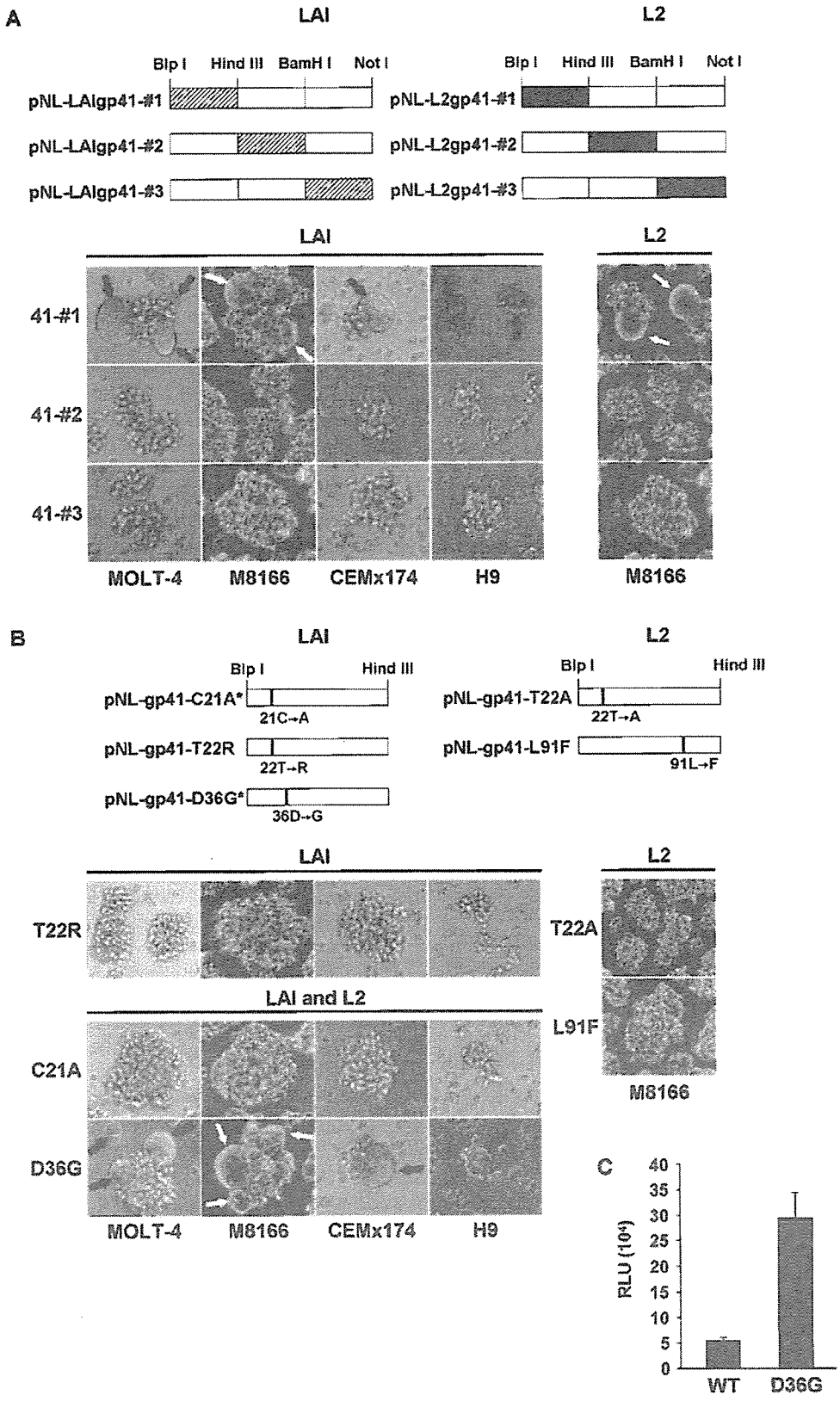

FIG. 2. Construction of gp41 recombinants and point mutants and their syncytium-forming activities and infectivities. (A) Chimeric viruses carrying three different regions of gp41 derived from pLAI or pL2 were constructed by utilizing the restriction enzyme sites BlpI, HindIII, BamHI and NotI. (B) Amino acid substitutions (21C→A, 22T→R, 22T→A, 36D→G, or 91L→F) were introduced within the BlpI-HindIII region of gp41 by site-directed mutagenesis. Asterisks show mutant constructs harboring a mutation commonly seen in both pLAI and pL2. The syncytium-formation assay (A and B) was performed as described for Fig. 1. Arrows indicate the formation of syncytia. (C) To determine infectivity, 5×10^5 MAGIC5A cells were infected with 10 ng of NL-Luc-envCT (WT) or NL-Luc-D36G (D36G), harboring the Luc gene in place of *nef*. After 48 h, cells were lysed and subjected to Luc assay. Averages from three independent experiments with standard deviations are indicated. RLU, relative light units.

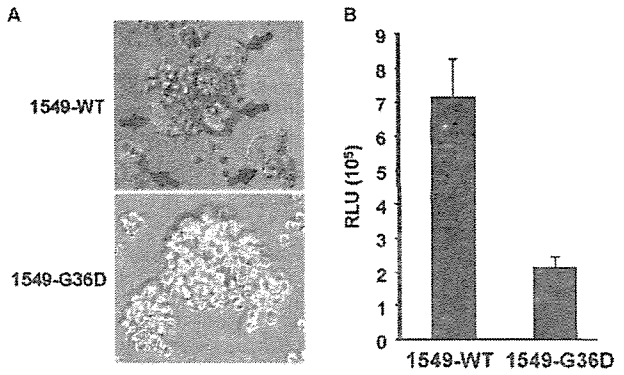

FIG. 3. Effect of the amino acid change at position 36 in gp41 in a primary-isolate-derived Env. (A) A syncytium formation assay was performed with MOLT-4 cells inoculated with NL-1549 (1549-WT) viruses carrying a primary-isolate (QH1549)-derived Env or with NL-1549-G36D (1549-G36D) viruses harboring the amino acid change 36G→D in 1549 gp41. Arrows indicate the formation of syncytia. (B) Infectivities of NL-Luc-1549 (1549-WT) and NL-Luc-1549-G36D (1549-G36D) viruses were measured by Luc assay as described for Fig. 2C. Averages from three independent experiments with standard deviations are indicated. RLU, relative light units.

tor cells, and equivalent levels of expression of WT and D36G Envs were confirmed by immunoblotting. As shown in Fig. 4A, the D36G Env enhanced Luc activity ~5-fold more than WT Env, consistent with microscopic observation of the fusion activity shown in Fig. 2B. In the viral binding assay, MAGIC5A cells were incubated with WT Env- and D36G Env-encoding viruses at 4°C, which is a temperature permissive for virus

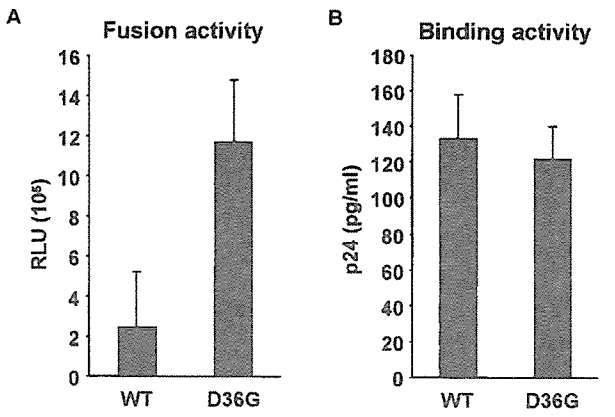

FIG. 4. Comparisons of cell-cell fusion (A) and viral binding (B) between WT and D36G mutant Envs. (A) 293T cells as the effector cells were transfected with pNLnΔBs (WT) or pNLnΔBs-D36G (D36G) and Tat expression plasmids, while MAGIC5A cells as the target cells were transfected with pLTR-hLucP+. Forty-eight hours later, both cell types were washed, trypsinized, and cocultured. After 5 h, cells were lysed and subjected to Luc assay. Averages from three independent experiments with standard deviations are indicated. RLU, relative light units. (B) MAGIC5A cells (1.5×10^6) were incubated with medium containing 100 ng of NL-Δenv, NL-envCT (WT), or NL-gp41-D36G (36G) viruses at 4°C. After 3 h, cells were extensively washed with ice-cold PBS three times and lysed with lysis buffer. Cell lysates were analyzed for p24 levels by ELISA. The background obtained with NL-Δenv viruses was subtracted from sample values. Averages from three independent experiments with standard deviations are indicated.

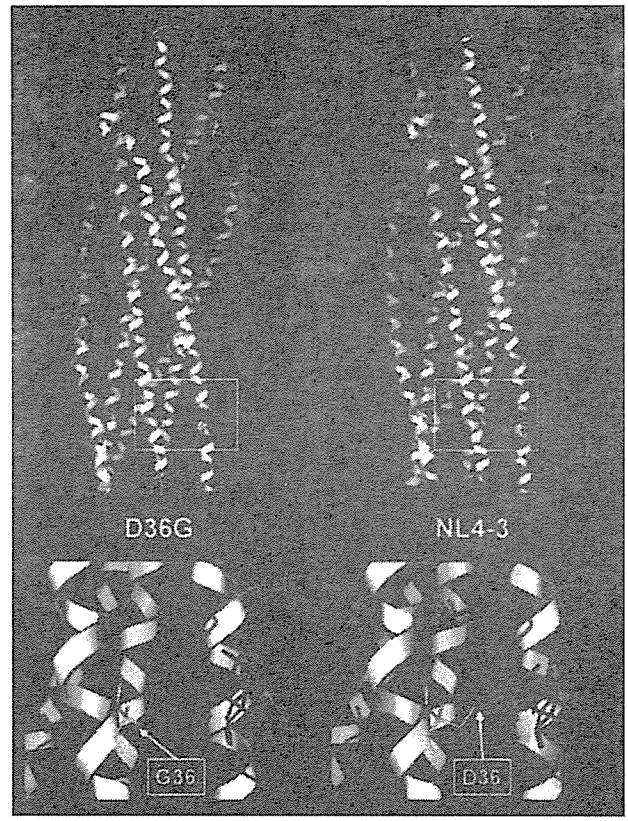

FIG. 5. Molecular modeling of HIV-1 gp41 ectodomain trimer. The 3-D model of an HIV-1 gp41 ectodomain trimer was constructed by the homology modeling technique using the MOE. HIV-1 gp41 ectodomain trimers of D36G (upper left) and NL4-3 (upper right) are displayed. Target portions of each trimer around amino acid position 36 are shown with side chains of position 36 in the N-peptide region and related amino acids within the C-peptide region. Arrows indicate the side chains of N and C helices of D36G (lower left) and NL4-3 gp41 (lower right).

binding but not internalization. After 3 h, unbound virions were removed by extensive washing, and cells were lysed and subjected to p24 ELISA. Background activity of the control virus (*env* defective), which showed ~30% of the binding activity of WT Env, was subtracted from the activity obtained for WT and D36G Envs. As shown in Fig. 4B, WT and D36G mutant viruses displayed equivalent levels of viral binding ability. We therefore conclude that the effect of the D36G amino acid substitution on syncytium formation results from an enhancement in fusogenic activity and not from enhanced virus binding due to an altered interaction between gp41 and gp120.

Comparison of the 3-D structure models of the gp41 ectodomain trimer. To more fully understand the mechanism by which fusogenicity differs between NL4-3 and the D36G mutant, we analyzed the effect of the D36G mutation on the predicted 3-D structure of the gp41 ectodomain trimer. Thermodynamically stable ectodomain structures of HIV-1 NL4-3 and its D36G mutant were constructed by homology modeling as described in Materials and Methods. As shown in Fig. 5, when the two structures were compared, it was obvious that the side chain of amino acid at position 36 in the N helix could affect the potential movement of the C helix of NL4-3 but not

that of the D36G mutant. The side chain of the aspartic acid in the NL4-3 (36D) model was shown to protrude toward the main chain of the C helix positioned in parallel with the N helix, being surrounded closely by the side chains of three amino acids in the C helix, i.e., Q141, K144, and N145. In such a structure, if the C helix moves vertically or horizontally during six-helix bundle formation, there could be a steric clash between the side chain of 36D and some of the three amino acids. In addition, the negatively charged 36D could induce distortion or incorrect positioning of the N and C helices by forming a misdirected salt bridge with K144, leading to a less stable helix structure. The positioning of the smaller, noncharged side chain of the glycine at position 36 in the D36G mutant model suggests that it would not clash with the side chains of the C helix during six-helix bundle formation. The model also predicts that the amino acid substitution at position 36 might cause a change in positioning of both the C and N helices per se. The mean distance between the main-chain backbones of the N and C helices was shorter in the D36G models than in the NL4-3 model (5.45 Å and 6.13 Å, respectively). Although the expected difference (about 0.7 Å) was in the range of RMSD between the predicted and actual structures, it was constantly observed with models made by different procedures, suggesting its intrinsic significance due to the difference of the size of side chain at position 36. Together, the data suggest that the substitution at position 36 with a charged, larger amino acid affects not only the local conformation of the helix but also the overall positioning of the two helices. Thus, the alteration of the amino acid at position 36 has a significant impact on determining the conformation of the N and C helices in the hairpin structure during membrane fusion.

DISCUSSION

In this study, we initially attempted to identify which region of the HIV-1 envelope protein could be responsible for the highly fusogenic activity that was observed in L2 viruses produced from MT-4 cells surviving after infection with LAI viruses (16, 20, 32). As a result of recombinational and mutational analyses based on pNL4-3, we found that a substitution of glycine (present in pL2/pLAI) for aspartic acid (present in pNL4-3) at position 36 of the ectodomain of gp41 was necessary and sufficient to confer robust syncytium-forming activity as well as enhanced infectivity. This phenomenon was confirmed by using a primary-isolate-derived Env protein with a glycine located at position 36 of this gp41 ectodomain. By performing quantitative fusion assays and viral binding assays, enhanced fusion activity was found not to be due to increased binding efficiency by altered gp41-mediated activity of gp120 but to be directly due to actual enhancement of viral fusion activity.

It is somewhat surprising that we could not determine any other key amino acid change which could display high fusion activity, since 36G of the gp41 ectodomain is conserved not only in pL2/pLAI but also in most other HIV-1 isolates (even in LAI/IIIB derivatives) and since one of the most widely used HIV-1 clones, pNL4-3, consisting of LAI/BRU at the 3′half, is rather exceptional, as first shown in the reports on T-20 (24, 35, 40, 42) (see below). Besides, one discrepancy remains in that although both L2 and LAI Envs harbor 36G in the ectodomain of gp41, L2 viruses are derived from the past virus stock of MT-4→MOLT-4-propagated strain LAI, which was not able to induce syncytium formation efficiently (32). It seems likely, however, that the majority of these polyclonal LAI preparations from MT-4/MOLT-4 cells might have carried 36D of gp41, which confers considerably less fusogenicity. We hypothesize that viruses carrying D36 in gp41 would take advantage of reduced fusogenic activity to lead to higher levels of viral propagation, since low-level cytopathic activity as a result of weak fusogenicity in D36 viruses might allow infected cells to survive longer than would G36 viruses. In terms of viral infectivity, D36 viruses should retain low but sufficient infectivity, as NL4-3 does. We therefore assume that D36 viruses might have dominated polyclonal LAI preparations from MT-4/MOLT-4 during the establishment of persistently infected cells. On the other hand, the reason why, despite the acquisition of high fusogenicity, L2-producing cells could survive after the in vitro acute phase of infection (20) might be that produced virions are replication defective because of the mutation in the protease gene and that the virus-producing cells have down-regulated CD4 from the cell surface, not allowing L2 virions to superinfect the cells.

The accuracy of the homology modeling is highly dependent on resolution of template structure for the modeling, as well as the degree of sequence similarity between the template and target proteins (2, 39). To obtain a high-quality gp41 ectodomain model, we used the 1QBZ structure, which was determined by X-ray crystallography analysis to have the best resolution (1.47 Å) and is the most accurate and complete structure of a retroviral gp41 ectodomain determined to date (48). Furthermore, 1QBZ has a sequence similarity of 52.5% to the target NL4-3 gp41 ectodomain, which is high enough to construct high-accuracy models with RMSDs of ~1 Å for the main chain between predicted and actual structures (2). Therefore, the gp41 ectodomain models presented here are likely to be highly accurate, predicting the six-helix bundle structure of each strain with an RSMD of ~1 Å for the main chain.

The comparison of the six-helix bundle models of NL4-3 and the D36G mutant revealed notable structural differences around amino acid position 36, which potentially the affect ability of the ectodomain to induce conformational change (Fig. 5). The models suggest that the NL4-3 ectodomain can be more refractory to the conformational changes than the D36G mutant ectodomain, because of more efficient steric clash and coulomb interaction between the N and C helix side chains (Fig. 5). This prediction is consistent with the experimental data indicating that the NL4-3 gp41 is less fusogenic than the gp41 with the D36G substitution (Fig. 1 to 4). Together, our data suggest that the amino acid at position 36 in the N helix is a critical regulator for the structural changes of the ectodomain.

Figure 6 shows a model of HIV-1 membrane fusion and the difference in fusion efficiency between 36D and 36G Envs. Binding of gp120 to CD4 and a chemokine receptor (not shown) leads to a conformational change in gp120 that alters the interactions of gp120 with gp41. This allows the gp41 fusion peptide to be exposed and to insert into the target cell membrane (Fig. 6, upper left) and allows the N-peptide region to form ân exposed trimeric coiled coil and the C-peptide region to be exposed as well (prehairpin intermediate shown in Fig. 6,

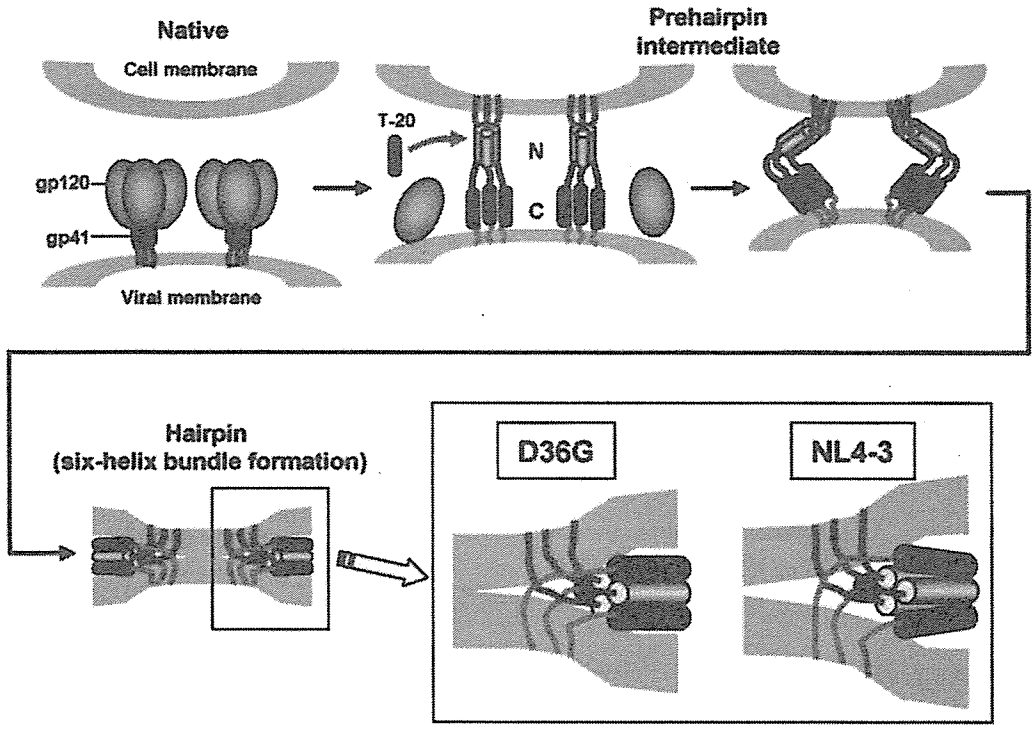

FIG. 6. A model of the HIV-1 Env-mediated fusion mechanism and a putative difference in hairpin formation between D36G and NL4-3 Envs. This model is adapted from that of Koshiba and Chan (22). Binding of gp120 to CD4 and a coreceptor (not shown) induces a conformational change in gp120 that allows exposure of gp41 fusion peptide (red) and its penetration into the target cellular membrane and allows the formation of the prehairpin intermediate (upper panel). As shown in the lower left panel, hairpin (six-helix bundle) formation occurs between trimeric N-peptide (gray) and C-peptide (blue) regions. Enlargements of putative six-helix bundles of D36G and NL4-3 gp41 ectodomains are displayed in the lower right panel.

upper middle and right). This intermediate is relatively long-lived and is vulnerable to C-peptide inhibitors such as T-20. When the C-peptide region is brought into close proximity to the N-peptide coiled coil and adopts a helical conformation, the prehairpin intermediate resolves to the fusion-active hairpin structure, which is a coiled coil composed of internal triple-stranded N-peptide helices paired with antiparallel outer C-peptide helices packed along hydrophobic grooves, forming a six-helix bundle. This rearrangement results in membrane apposition (Fig. 6, lower left). As shown in the lower right panel of Fig. 6, while the D36G mutant, which can be considered a consensus gp41, undergoes the normal six-helix bundle formation, NL4-3 carrying 36D in gp41 faces physical impediments to this formation since the protrusion of the negatively charged 36D residue in the N helix toward the C helix would induce a steric clash between the N and C helices, a salt bridge with 36D and K144 in the C helix, and an extended distance between the main-chain backbones of the N and C helices.

T-20 is a 36-amino-acid synthetic peptide that is homologous to the last 36 amino acids of the C-peptide helix (8, 27, 45) in the ectodomain of gp41. By competitively binding the N-peptide helix (Fig. 6, upper middle), T-20 blocks formation of the hairpin structure necessary for membrane fusion. Studies in vitro have shown that T-20 prevents cell-free HIV-1 infection and virus-mediated cell-cell fusion (35, 40). After in vitro passage in the presence of increasing concentrations of T-20, resistant variants of HIV-1_{IIIB} developed mutations at positions 36 and 38 (G to D or S and V to M) (35). Also, sequence analysis in vivo indicated that T-20-resistant viruses frequently and specifically contained mutations at position 36 (G to D), leading to a marked decrease in susceptibility to T-20 inhibition (42). These findings were supported by mutational evidence that compared with NL-D36G viruses (NL4-3 altered to match the consensus sequence at position 36), native NL4-3 (36D) displayed eightfold reduction in T-20 sensitivity (17). This is intriguing in that the position of the mutation observed in the T-20 escape mutants is exactly equivalent to that of the target mutation in our study. Just as observed in our experiments, the mutation which naturally occurs in the viruses escaping from T-20 is expected to induce a reduction in fusion activity, but the mutants still retain infectibility as high as that of NL4-3 viruses. Our findings, therefore, imply that the phenotypic and structural differences between fusogenic and nonfusogenic viruses described in this paper may reflect those between T-20-sensitive and nonsensitive viruses and furthermore suggest that the 36D mutation observed in T-20-resistant mutants might reduce the T-20 binding efficiency by the same mechanism as discussed above.

Considerable work on gp41 through mutagenesis studies and escape variants arising from T-20 selective pressure with the alterations in virus replication kinetics has indicated that other positions of gp41 also regulate the fusogenicity. Among gp41 mutants reported so far, many of the gp41 mutations leading to reduced fusion activity are located within or in the proximity of the "deep pocket" (6), such as L54, L55, L57, V59, W60, G61, I62, W117, W120, and I124 (4, 9, 11, 14, 25, 34, 41, 44). Since

the mutations of these conserved residues required for the six-helix bundle formation abolish viral replication (29), this pocket could be a good target for T-1249, the second fusion inhibitor, whose binding region extends into the deep pocket (13). The W85M mutation, located in the side of disulfide-bonded loop, confers impaired fusogenicity but wild-type infectivity (4). Among several mutations which have been reported to impair the fusogenicity and are located in the T-20 target region, such as I37, Q40, L45, and I48 (4, 8, 14, 25), naturally occurring mutations in the presence of T-20 are found in I37 and L45 in addition to G36 (whose phenotype was first described in this study). Fusion phenotypes of other mutants seen in T-20 resistance in vivo and in vitro (Q32, V38, and Q39) are undetermined (27, 28, 35, 42).

In conclusion, our data indicate that amino acid 36 in the gp41 ectodomain, which is conserved in nearly all HIV-1 isolates except for NL4-3 and T-20 escape viruses, controls the fusogenic activity and that structural impediment in the gp41 ectodomain of NL4-3 and T-20 escape viruses may lead to the inefficient membrane fusion. Further studies will be required to fully understand the mechanism by which viruses acquire resistance to the T-20 fusion inhibitor.

ACKNOWLEDGMENTS

We are grateful to David Chan for giving us permission to use and modify Fig. 6 and for critical reading of the manuscript, to Bryan R. Cullen for helpful discussion, and to Masashi Tatsumi for providing MAGIC5A cells.

This work was supported in part by a grant from the Ministry of Education, Science, Technology, Sports and Culture of Japan and by a grant from the Ministry of Health, Labor and Welfare of Japan.

REFERENCES

1. **Adachi, A., H. E. Gendelman, S. Koenig, T. Folks, R. Willey, A. Rabson, and M. A. Martin.** 1986. Production of acquired immunodeficiency syndrome-associated retrovirus in human and nonhuman cells transfected with an infectious molecular clone. J. Virol. **59**:284–291.
2. **Baker, D., and A. Sali.** 2001. Protein structure prediction and structural genomics. Science **294**:93–96.
3. **Caffrey, M., M. Cai, J. Kaufman, S. J. Stahl, P. T. Wingfield, D. G. Covell, A. M. Gronenborn, and G. M. Clore.** 1998. Three-dimensional solution structure of the 44 kDa ectodomain of SIV gp41. EMBO J. **17**:4572–4584.
4. **Cao, J., L. Bergeron, E. Helseth, M. Thali, H. Repke, and J. Sodroski.** 1993. Effects of amino acid changes in the extracellular domain of the human immunodeficiency virus type 1 gp41 envelope glycoprotein. J. Virol. **67**:2747–2755.
5. **Cao, J., B. Vasir, and J. G. Sodroski.** 1994. Changes in the cytopathic effects of human immunodeficiency virus type 1 associated with a single amino acid alteration in the ectodomain of the gp41 transmembrane glycoprotein. J. Virol. **68**:4662–4668.
6. **Chan, D. C., D. Fass, J. M. Berger, and P. S. Kim.** 1997. Core structure of gp41 from the HIV envelope glycoprotein. Cell **89**:263–273.
7. **Chan, D. C., and P. S. Kim.** 1998. HIV entry and its inhibition. Cell **93**:681–684.
8. **Chen, C. H., T. J. Matthews, C. B. McDanal, D. P. Bolognesi, and M. L. Greenberg.** 1995. A molecular clasp in the human immunodeficiency virus (HIV) type 1 TM protein determines the anti-HIV activity of gp41 derivatives: implication for viral fusion. J. Virol. **69**:3771–3777.
9. **Chen, S. S., C. N. Lee, W. R. Lee, K. McIntosh, and T. H. Lee.** 1993. Mutational analysis of the leucine zipper-like motif of the human immunodeficiency virus type 1 envelope transmembrane glycoprotein. J. Virol. **67**:3615–3619.
10. **Decroly, E., M. Vandenbranden, J. M. Ruysschaert, J. Cogniaux, G. S. Jacob, S. C. Howard, G. Marshall, A. Kompelli, A. Basak, F. Jean, and et al.** 1994. The convertases furin and PC1 can both cleave the human immunodeficiency virus (HIV)-1 envelope glycoprotein gp160 into gp120 (HIV-1 SU) and gp41 (HIV-I TM). J. Biol. Chem. **269**:12240–12247.
11. **Dubay, J. W., S. J. Roberts, B. Brody, and E. Hunter.** 1992. Mutations in the leucine zipper of the human immunodeficiency virus type 1 transmembrane glycoprotein affect fusion and infectivity. J. Virol. **66**:4748–4756.
12. **Dubay, J. W., S. J. Roberts, B. H. Hahn, and E. Hunter.** 1992. Truncation of the human immunodeficiency virus type 1 transmembrane glycoprotein cytoplasmic domain blocks virus infectivity. J. Virol. **66**:6616–6625.
13. **Eron, J. J., R. M. Gulick, J. A. Bartlett, T. Merigan, R. Arduino, J. M. Kilby, B. Yangco, A. Diers, C. Drobnes, R. DeMasi, M. Greenberg, T. Melby, C. Raskino, P. Rusnak, Y. Zhang, R. Spence, and G. D. Miralles.** 2004. Short-term safety and antiretroviral activity of T-1249, a second-generation fusion inhibitor of HIV. J. Infect. Dis. **189**:1075–1083.
14. **Follis, K. E., S. J. Larson, M. Lu, and J. H. Nunberg.** 2002. Genetic evidence that interhelical packing interactions in the gp41 core are critical for transition of the human immunodeficiency virus type 1 envelope glycoprotein to the fusion-active state. J. Virol. **76**:7356–7362.
15. **Freed, E. O., D. J. Myers, and R. Risser.** 1990. Characterization of the fusion domain of the human immunodeficiency virus type 1 envelope glycoprotein gp41. Proc. Natl. Acad. Sci. USA **87**:4650–4654.
16. **Goto, T., K. Ikuta, J. J. Zhang, C. Morita, K. Sano, M. Komatsu, H. Fujita, S. Kato, and M. Nakai.** 1990. The budding of defective human immunodeficiency virus type 1 (HIV-1) particles from cell clones persistently infected with HIV-1. Arch. Virol. **111**:87–101.
17. **Greenberg, M. L., and N. Cammack.** 2004. Resistance to enfuvirtide, the first HIV fusion inhibitor. J. Antimicrob. Chemother. **54**:333–340.
18. **Hallenberger, S., V. Bosch, H. Angliker, E. Shaw, H. D. Klenk, and W. Garten.** 1992. Inhibition of furin-mediated cleavage activation of HIV-1 glycoprotein gp160. Nature **360**:358–361.
19. **Helseth, E., U. Olshevsky, D. Gabuzda, B. Ardman, W. Haseltine, and J. Sodroski.** 1990. Changes in the transmembrane region of the human immunodeficiency virus type 1 gp41 envelope glycoprotein affect membrane fusion. J. Virol. **64**:6314–6318.
20. **Ikuta, K., C. Morita, M. Nakai, N. Yamamoto, and S. Kato.** 1988. Defective human immunodeficiency virus (HIV) particles produced by cloned cells of HTLV-I-carrying MT-4 cells persistently infected with HIV. Jpn. J. Cancer Res. **79**:418–423.
21. **Kinomoto, M., T. Mukai, Y. G. Li, Y. Iwabu, J. Warachit, J. A. Palacios, M. S. Ibrahim, S. Tsuji, T. Goto, and K. Ikuta.** 2004. Enhancement of human immunodeficiency virus type 1 infectivity by replacing the region including Env derived from defective particles with an ability to form particle-mediated syncytia in CD4+T cells. Microbes Infect. **6**:911–918.
22. **Koshiba, T., and D. C. Chan.** 2003. The prefusogenic intermediate of HIV-1 gp41 contains exposed C-peptide regions. J. Biol. Chem. **278**:7573–7579.
23. **Kwong, P. D., R. Wyatt, J. Robinson, R. W. Sweet, J. Sodroski, and W. A. Hendrickson.** 1998. Structure of an HIV gp120 envelope glycoprotein in complex with the CD4 receptor and a neutralizing human antibody. Nature **393**:648–659.
24. **Lu, J., P. Sista, F. Giguel, M. Greenberg, and D. R. Kuritzkes.** 2004. Relative replicative fitness of human immunodeficiency virus type 1 mutants resistant to enfuvirtide (T-20). J. Virol. **78**:4628–4637.
25. **Lu, M., M. O. Stoller, S. Wang, J. Liu, M. B. Fagan, and J. H. Nunberg.** 2001. Structural and functional analysis of interhelical interactions in the human immunodeficiency virus type 1 gp41 envelope glycoprotein by alanine-scanning mutagenesis. J. Virol. **75**:11146–11156.
26. **Malashkevich, V. N., D. C. Chan, C. T. Chutkowski, and P. S. Kim.** 1998. Crystal structure of the simian immunodeficiency virus (SIV) gp41 core: conserved helical interactions underlie the broad inhibitory activity of gp41 peptides. Proc. Natl. Acad. Sci. USA **95**:9134–9139.
27. **Matthews, T., M. Salgo, M. Greenberg, J. Chung, R. DeMasi, and D. Bolognesi.** 2004. Enfuvirtide: the first therapy to inhibit the entry of HIV-1 into host CD4 lymphocytes. Nat. Rev. Drug Discov. **3**:215–225.
28. **Menzo, S., A. Castagna, A. Monachetti, H. Hasson, A. Danise, E. Carini, P. Bagnarelli, A. Lazzarin, and M. Clementi.** 2004. Genotype and phenotype patterns of human immunodeficiency virus type 1 resistance to enfuvirtide during long-term treatment. Antimicrob. Agents Chemother. **48**:3253–3259.
29. **Mo, H., A. K. Konstantinidis, K. D. Stewart, T. Dekhtyar, T. Ng, K. Swift, E. D. Matayoshi, W. Kati, W. Kohlbrenner, and A. Molla.** 2004. Conserved residues in the coiled-coil pocket of human immunodeficiency virus type 1 gp41 are essential for viral replication and interhelical interaction. Virology **329**:319–327.
30. **Mochizuki, N., N. Otsuka, K. Matsuo, T. Shiino, A. Kojima, T. Kurata, K. Sakai, N. Yamamoto, S. Isomura, T. N. Dhole, Y. Takebe, M. Matsuda, and M. Tatsumi.** 1999. An infectious DNA clone of HIV type 1 subtype C. AIDS Res. Hum. Retroviruses **15**:1321–1324.
31. **Morikawa, Y., E. Barsov, and I. Jones.** 1993. Legitimate and illegitimate cleavage of human immunodeficiency virus glycoproteins by furin. J. Virol. **67**:3601–3604.
32. **Ohki, K., Y. Kishi, Y. Nishino, M. Sumiya, T. Kimura, T. Goto, M. Nakai, and K. Ikuta.** 1991. Noninfectious doughnut-shaped human immunodeficiency virus type 1 can induce syncytia mediated by fusion of the particles with CD4-positive cells. J. Acquir. Immune Defic. Syndr. **4**:1233–1240.
33. **Owens, R. J., C. Burke, and J. K. Rose.** 1994. Mutations in the membrane-spanning domain of the human immunodeficiency virus envelope glycoprotein that affect fusion activity. J. Virol. **68**:570–574.
34. **Perrin, C., E. Fenouillet, and I. M. Jones.** 1998. Role of gp41 glycosylation sites in the biological activity of human immunodeficiency virus type 1 envelope glycoprotein. Virology **242**:338–345.

35. **Rimsky, L. T., D. C. Shugars, and T. J. Matthews.** 1998. Determinants of human immunodeficiency virus type 1 resistance to gp41-derived inhibitory peptides. J. Virol. **72:**986–993.
36. **Tan, K., J. Liu, J. Wang, S. Shen, and M. Lu.** 1997. Atomic structure of a thermostable subdomain of HIV-1 gp41. Proc. Natl. Acad. Sci. USA **94:** 12303–12308.
37. **Tokunaga, K., M. L. Greenberg, M. A. Morse, R. I. Cumming, H. K. Lyerly, and B. R. Cullen.** 2001. Molecular basis for cell tropism of CXCR4-dependent human immunodeficiency virus type 1 isolates. J. Virol. **75:**6776–6785.
38. **Tokunaga, K., A. Kojima, T. Kurata, K. Ikuta, H. Akari, A. H. Koyama, M. Kawamura, R. Inubushi, R. Shimano, and A. Adachi.** 1998. Enhancement of human immunodeficiency virus type 1 infectivity by Nef is producer cell-dependent. J. Gen. Virol. **79:**2447–2453.
39. **Tramontano, A.** 1998. Homology modeling with low sequence identity. Methods **14:**293–300.
40. **Trivedi, V. D., S. F. Cheng, C. W. Wu, R. Karthikeyan, C. J. Chen, and D. K. Chang.** 2003. The LLSGIV stretch of the N-terminal region of HIV-1 gp41 is critical for binding to a model peptide, T20. Protein Eng. **16:**311–317.
41. **Wang, S., J. York, W. Shu, M. O. Stoller, J. H. Nunberg, and M. Lu.** 2002. Interhelical interactions in the gp41 core: implications for activation of HIV-1 membrane fusion. Biochemistry **41:**7283–7292.
42. **Wei, X., J. M. Decker, H. Liu, Z. Zhang, R. B. Arani, J. M. Kilby, M. S. Saag, X. Wu, G. M. Shaw, and J. C. Kappes.** 2002. Emergence of resistant human immunodeficiency virus type 1 in patients receiving fusion inhibitor (T-20) monotherapy. Antimicrob. Agents Chemother. **46:**1896–1905.
43. **Weissenhorn, W., A. Dessen, S. C. Harrison, J. J. Skehel, and D. C. Wiley.** 1997. Atomic structure of the ectodomain from HIV-1 gp41. Nature **387:** 426–430.
44. **Weng, Y., and C. D. Weiss.** 1998. Mutational analysis of residues in the coiled-coil domain of human immunodeficiency virus type 1 transmembrane protein gp41. J. Virol. **72:**9676–9682.
45. **Wild, C. T., D. C. Shugars, T. K. Greenwell, C. B. McDanal, and T. J. Matthews.** 1994. Peptides corresponding to a predictive alpha-helical domain of human immunodeficiency virus type 1 gp41 are potent inhibitors of virus infection. Proc. Natl. Acad. Sci. USA **91:**9770–9774.
46. **Willey, R. L., J. S. Bonifacino, B. J. Potts, M. A. Martin, and R. D. Klausner.** 1988. Biosynthesis, cleavage, and degradation of the human immunodeficiency virus 1 envelope glycoprotein gp160. Proc. Natl. Acad. Sci. USA **85:**9580–9584.
47. **Wu, L., N. P. Gerard, R. Wyatt, H. Choe, C. Parolin, N. Ruffing, A. Borsetti, A. A. Cardoso, E. Desjardin, W. Newman, C. Gerard, and J. Sodroski.** 1996. CD4-induced interaction of primary HIV-1 gp120 glycoproteins with the chemokine receptor CCR-5. Nature **384:**179–183.
48. **Yang, Z. N., T. C. Mueser, J. Kaufman, S. J. Stahl, P. T. Wingfield, and C. C. Hyde.** 1999. The crystal structure of the SIV gp41 ectodomain at 1.47 A resolution. J. Struct. Biol. **126:**131–144.

Cellular Microbiology (2007) 9(1), 196–203

doi:10.1111/j.1462-5822.2006.00781.x
First published online 10 August 2006

A broad antiviral neutral glycolipid, fattiviracin FV-8, is a membrane fluidity modulator

Shinji Harada,[1]* Kazumi Yokomizo,[2] Kazuaki Monde,[1] Yosuke Maeda[1] and Keisuke Yusa[1]

[1]*Department of Medical Virology, Graduate School of Medical Sciences, Kumamoto University, Kumamoto 860-8556, Japan.*

[2]*Faculty of Pharmaceutical Science, Sojo University, Kumamoto 860-0082, Japan.*

Summary

To screen for an effective antiviral compound which acts as a membrane fluidity modulator, dichotomous effects on human immunodeficiency virus type 1 (HIV-1) infection due to different treatments of several glycolipids and lipids were examined. Continuous treatment of infected cells with 40 μg ml^{-1} fattiviracin FV-8, a neutral glycolipid isolated from *Streptomycetes*, inhibited HIV-1 infection by 96%, whereas pretreatment with 400 μg ml^{-1} enhanced infectivity 4.7-fold. The glycolipid showed similar effects as glycyrrhizin; it inhibited infection by broad enveloped viruses, blocked cell–cell fusion, reduced the infectivity of treated virions and enhanced susceptibility to viral infection and cell–cell fusion of cells pretreated with high doses of the compound. Suppression and enhancement was correlated with decreased and increased fluidity of plasma membrane of the fattiviracin FV-8-treated cells. Restricted movement of membrane molecules might impede the formation of a wide fusion pore, and therefore be critical to the entry of viruses. Thus, this can be applied as a new strategy to inhibit viral infections.

Introduction

Fusion is used by many enveloped viruses to gain entry into cells. Fusion actually encompasses many different processes, such as conformational changes of the viral glycoprotein spike by binding to receptor(s) or low pH in the endosome, exposing hydrophobic fusion peptides (fusion-activated domain) and trimers formed from helical coiled-coil rods (Colman and Lawrence, 2003) or a β-sheet loop (Gibbons *et al.*, 2004; Modis *et al.*, 2004). One of the common fusion processes among enveloped viruses is fluidity-mediated accumulation of fusion-activated domains whereby the plasma membrane and viral envelope form a wide fusion pore large enough for a viral core to pass through (Plonsky and Zimmerberg, 1996; Roche and Gaudin, 2002; Gibbons *et al.*, 2003; Harada *et al.*, 2004a,b).

Correlation between HIV-1 infectivity and membrane fluidity was observed; namely a 5% decrease in fluidity suppressed HIV-1 infectivity by 56%, whereas a 5% increase enhanced infectivity 2.4-fold (Harada *et al.*, 2005). Glycyrrhizin with hydrophilic and lipophilic domains decreased or increased membrane fluidity depending on continuous treatment or pretreatment, respectively, of cells, which correlated with suppression or enhancement of HIV-1 infectivity and cell–cell fusion activity (Harada, 2005). Glycyrrhizin acts as a fluidity modulator probably due to its simple diffusion in and out of lipid bilayer membranes, thus showing broad antiviral activity especially against enveloped viruses. However, a disadvantage of the glycyrrhizin is that a high concentration (500 μg ml^{-1}) of the compound is needed to suppress viral infections. Thus, a more effective modulator is required.

It is hypothesized that glycolipids could exert the same pharmacodynamic action on the lipid bilayer membrane as glycyrrhizin, because glycolipids are amphipathic with hydrophilic sugar and lipophilic lipid structures. In order to evaluate the effectiveness of a number of compounds in blocking HIV-1 infection by decreasing membrane fluidity, it was necessary to develop a screening system, which was highly reproducible and convenient for parallel evaluation. In this paper, we screened accessible glycolipid compounds as membrane fluidity modulators to seek an effective antiviral agent and used lipids as a control. We found one (fattiviracin FV-8) consisting of high-molecular-weight glycolipids that showed strong anti-HIV-1 activity by suppressing membrane fluidity. We propose that some of the glycolipids could be used as antiviral agents through a new mechanism of blocking fusion-pore-formation.

Received 16 March, 2006; revised 8 June, 2006; accepted 29 June, 2006. *For correspondence. E-mail biodef@gpo.kumamoto-u.ac.jp; Tel. (+81) 96 3735128; Fax (+81) 96 3735132.

Table 1. Effect of lipids and glycolipids on HIV-1 infection.

Agents (MW)	% infection[a] of X4 HIV-1 by	
	Pretreatment of cells[b]	Continuous treatment[c]
I. Lipids		
Sphingomyelin	NT	> 80
Sphingosine	NT	> 80
Lysophosphatidic acid	< 120	> 80
II. Glycolipids		
Galactosylceramide (< 920)	200	70
Monosialoganglioside GM_1	< 120	66
Capsianoside II (1084)	143	61
Capsianoside XI (922)	150	78
Capsianoside G (1402)	819	9
Capsianoside A (1562)	210	43
Fattiviracin FV-8 (1432)	473	4

a. Percentage infection; (% positive cells in test/% positive cells in control) × 100.
b. 400 μg ml^{-1} of each agent was used.
c. 40 μg ml^{-1} of each agent was used.
NT; not tested.

Results and discussion

Screening of lipids and glycolipids as membrane fluidity modulators

As dichotomous (inhibitory and enhanced) effects of glycyrrhizin on HIV-1 infection well reflected changes in membrane fluidity (Harada, 2005) and could be conveniently assessed by infection of MAGI/CCR5 cells with LAI (X4) HIV-1, a number of lipids and glycolipids were screened with this system (Table 1). The cells were mixed with viruses and 40 μg ml^{-1} of each compound, cultured for 2 days (continuous treatment) and were stained to detect HIV-1-positive cells by multinuclear activation of a galactosidase indicator (MAGI) assay (Kimpton and Emerman, 1992). Table 1 shows that the lipids had no effect (less than 20% inhibition), while glycolipids exhibited 22–96% inhibition of HIV-1 infection. Capsianosides were extracted from *Capsicum annuum*. Capsianosides II and XI were identified as monomeric compounds of acylic diterpene glycoside, and G and A as esters of the acylic diterpene glycoside (Song *et al.*, 2001). Capsianosides II and A have a longer glucose chain than XI and G. A neutral glycolipid, named fattiviracin FV-8 that was isolated from *Streptomycetes* is a macrocyclic diester consisting of four D-glucose units and two (C_{24} and C_{33}) hydroxy fatty acids (Uyeda *et al.*, 1998). Fattiviracin FV-8 has the same macrocyclic diester structure as cycloviracins B_1 and B_2 (Tsunakawa *et al.*, 1992a,b). When the cells were treated with 400 μg ml^{-1} of each glycolipid at 37°C for 1 h, washed once with medium (pretreatment) and subjected to HIV-1 infection, all except monosialoganglioside GM_1 showed enhanced susceptibility to HIV-1 infection. Among them, compounds with higher molecular weight and fewer sugars (e.g. capsianoside G and fattiviracin FV-8) tended to exhibit more inhibitory and stimulatory effects on HIV-1 infection. In particular, fattiviracin FV-8 showed 96% inhibition and 4.7-fold enhancement of HIV-1 infectivity. Thus, we further explored and clarified how fattiviracin FV-8 acts on HIV-1 infection.

Inhibitory effects of fattiviracin FV-8 on HIV-1 infection by continuous treatment

Fattiviracin FV-8 has been reported to show potent antiviral activity against herpes simplex virus, varicella-zoster virus and influenza A virus as well as HIV-1 (Yokomizo *et al.*, 1998; Habib *et al.*, 2001). The effect of fattiviracin FV-8 on LAI (X4), JR-FL (R5) and 89.6 (X4R5) HIV-1 infection was reassessed when MAGI/CCR5 cells were treated with mixtures of each virus with the diluted glycolipid. The compound inhibited all strains in a dose-dependent manner; 50% and 90% effective concentrations (EC_{50} and EC_{90}) to each strain were observed at about 6.25 μg ml^{-1} and 25 μg ml^{-1} respectively (Fig. 1A). Therefore, the inhibitory effect of the fattiviracin FV-8 was not dependent on the viral strain. The concentration required to inhibit 50% of MAGI/CCR5 cell growth (CC_{50}) by continuous treatment was 280 μg ml^{-1}. Fattiviracin FV-8 weakly inhibited viral adsorption dose-dependently (Fig. 1B) by measuring the amount of p24 bound on cells. Fifty per cent inhibition of viral binding to cells occurred at 50 μg ml^{-1}, at which concentration more than 95% of viral infection was inhibited (Fig. 1A). Thus, inhibition of viral attachment by fattiviracin FV-8 was not parallel to the inhibition of viral infectivity. To analyse the time-dependent effect of fattiviracin FV-8, the glycolipid was added at 0, 1 and 3 h after inoculation of X4 HIV-1 to MAGI/CCR5 cells to obtain a final concentration of 12.5 μg ml^{-1}. The per cent infection at 0, 1 and 3 h were 16.5%, 66.0% and 87.8% respectively (Fig. 1C). As we previously reported (Habib *et al.*,

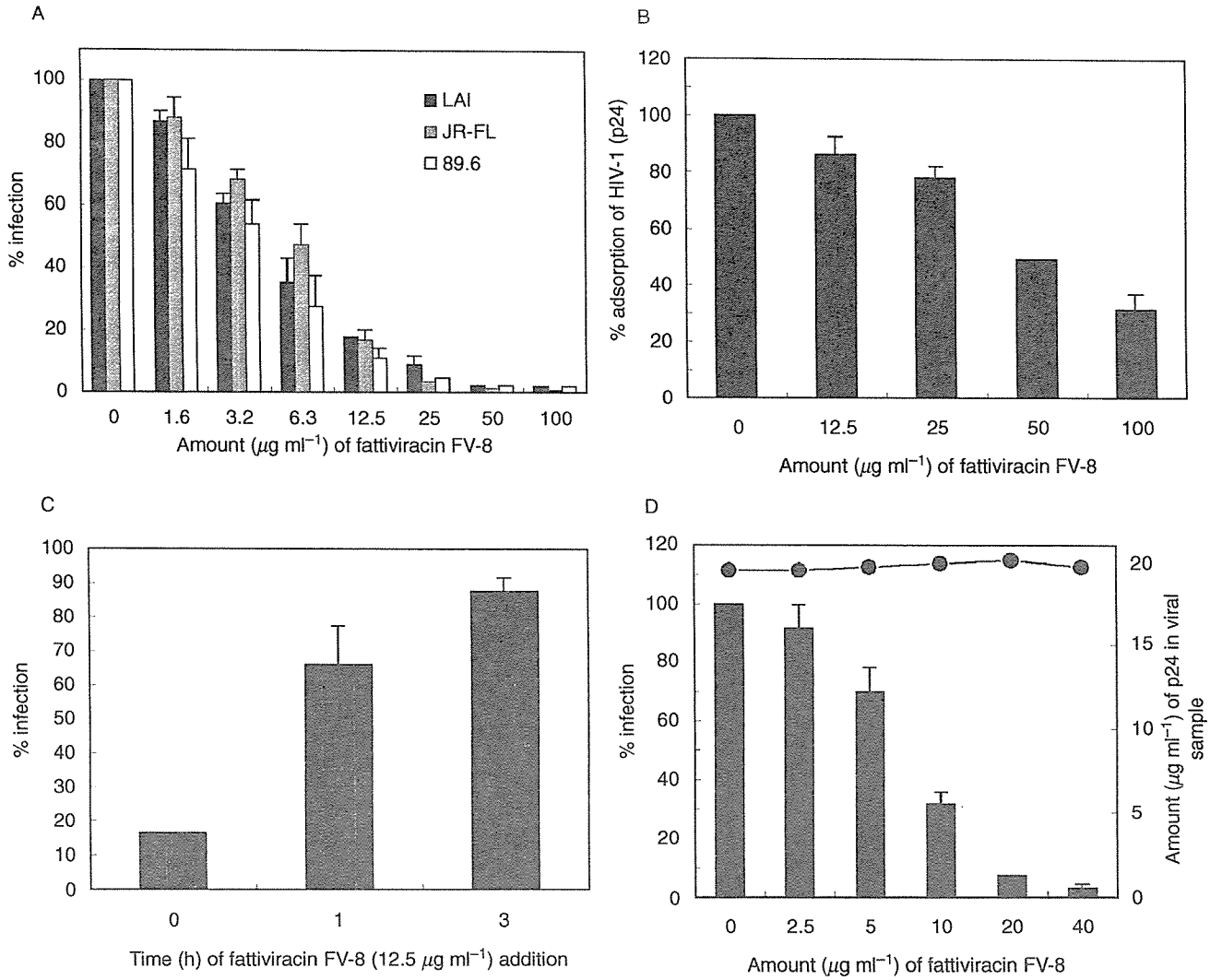

Fig. 1. Inhibitory effects of fattiviracin FV-8 on HIV-1 infection.
A. MAGI/CCR5 cells were infected with LAI, JR-FL and 89.6 viruses in the presence of serially diluted fattiviracin FV-8 in triplicate.
B. MAGI/CCR5 cells were incubated with LAI viruses at 37°C for 1 h in triplicate and washed twice with PBS. The amount of adsorbed viruses was assessed by p24 ELISA.
C. MAGI/CCR5 cells were infected with LAI viruses and fattiviracin FV-8 was added at 0, 1 and 3 h to obtain a final concentration of 12.5 μg ml^{-1}. The experiments were performed in triplicate.
D. LAI viruses in supernatants were treated with serially diluted fattiviracin FV-8. Each treated viral preparation after removing the excess glycolipid was subjected to determination of the p24 amount (line) and infectivity in triplicate (bar). Bars show the mean ± SD.

2001), fattiviracin FV-8 was most effective against HIV-1 infection when the compound was added during viral adsorption for 1 h, indicating that the glycolipid inhibited the early phase of the HIV-1 replication cycle after attachment. We further confirmed that direct treatment of X4 HIV-1 with serially diluted fattiviracin FV-8 for 1 h at 37°C reduced its infectivity dose-dependently and the EC_{50} was about 7.5 μg ml^{-1} (Fig. 1D). As the p24 amount of each viral preparation treated with fattiviracin FV-8 was unchanged at about 20 ng ml^{-1} (Fig. 1D), the glycolipid inhibited viral infection particularly not by lysing the viral particles.

Enhanced effects of fattiviracin FV-8 on HIV-1 infection by pretreatment of cells and effects on cell–cell fusion

The MAGI/CCR5 cells were treated with 200–800 μg ml^{-1} fattiviracin FV-8 for 1 h at 37°C and washed with medium. The glycolipid-pretreated cells were then infected with LAI, JR-FL and 89.6 strains of HIV-1 to assess their infectivity. Figure 2A shows that the infectivity of each virus increased six to eight times when the cells were pretreated with 600 μg ml^{-1} of fattiviracin FV-8. No significant effect was observed by the pretreatment with less than 50 μg ml^{-1}. The amount of adsorbed X4 viruses was

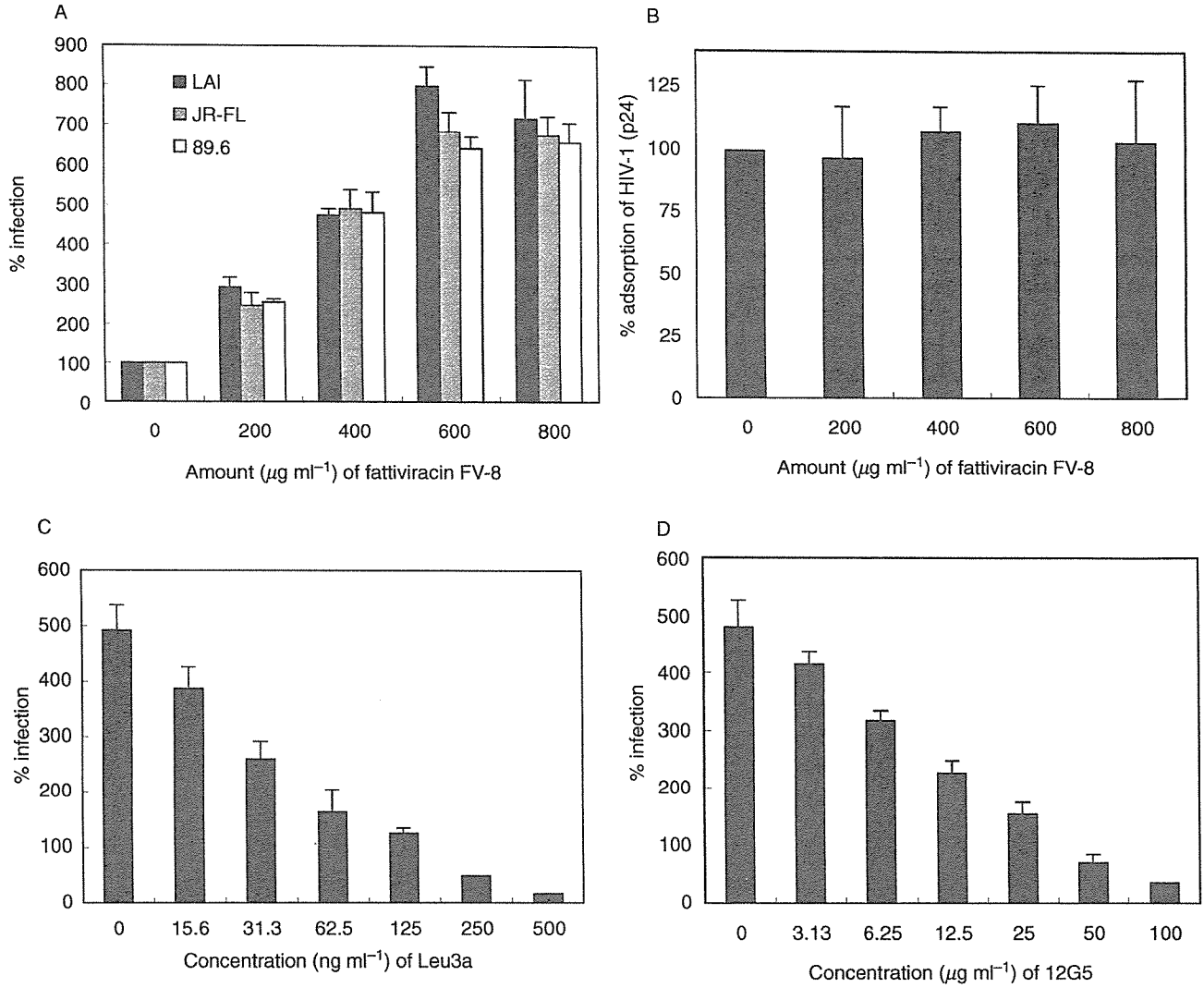

Fig. 2. Enhanced effects of fattiviracin FV-8 on HIV-1 infection.
A. MAGI/CCR5 cells were treated with serially diluted fattiviracin FV-8 at 37°C for 1 h and washed once with medium. Then, the pretreated cells were infected with LAI, JR-FL and 89.6 viruses in triplicate.
B. The fattiviracin FV-8-pretreated MAGI/CCR5 cells as in (A) were incubated with LAI viruses at 37°C for 1 h in triplicate and washed twice with PBS. The amount of adsorbed virus was assessed by p24 ELISA.
C. MAGI/CCR5 cells pretreated with 400 μg ml^{-1} fattiviracin FV-8 were infected with LAI viruses in the presence of serially diluted Leu 3a mAb in triplicate.
D. MAGI/CCR5 cells pretreated with 400 μg ml^{-1} fattiviracin FV-8 were infected with LAI viruses in the presence of serially diluted 12G5 mAb in triplicate. Bars show the mean ± SD.

not affected even though the cells were pretreated with 800 μg ml^{-1} of fattiviracin FV-8 (Fig. 2B). Fattiviracin FV-8 did not enhance the expression of CD4 nor CXCR4 by FACS analysis (data not shown). The enhanced infectivity of LAI HIV-1 by pretreatment of the cells is not a consequence of more viral adsorption (Fig. 2B), suggesting that the pretreatment of fattiviracin FV-8 may enhance the fusion step of viral entry. This enhancement was dose-dependently blocked by Leu 3a (Fig. 2C) and 12G5 (Fig. 2D) monoclonal antibodies, indicating that the increased infectivity was mediated by or depended on the amount of CD4 and CXCR4 molecules involved in fusion. The enhancement could result from accumulation of receptors at the site of viral attachment.

Next, the effect of fattiviracin FV-8 on cell–cell fusion was examined by coculturing chronically HIV-1 infected MOLT-4 (MOLT-4/HIV-1_{C-2}) cells with uninfected MOLT-4 cells (Fig. S1A) for 24 h. Fusion, which may relate to virological synapse (McDonald *et al.*, 2003), was completely inhibited by adding 20 μg ml^{-1} fattiviracin FV-8 to culture medium (Fig. S1B). When the MOLT-4/HIV-1_{C-2} cells were cocultured with target MOLT-4 cells pretreated

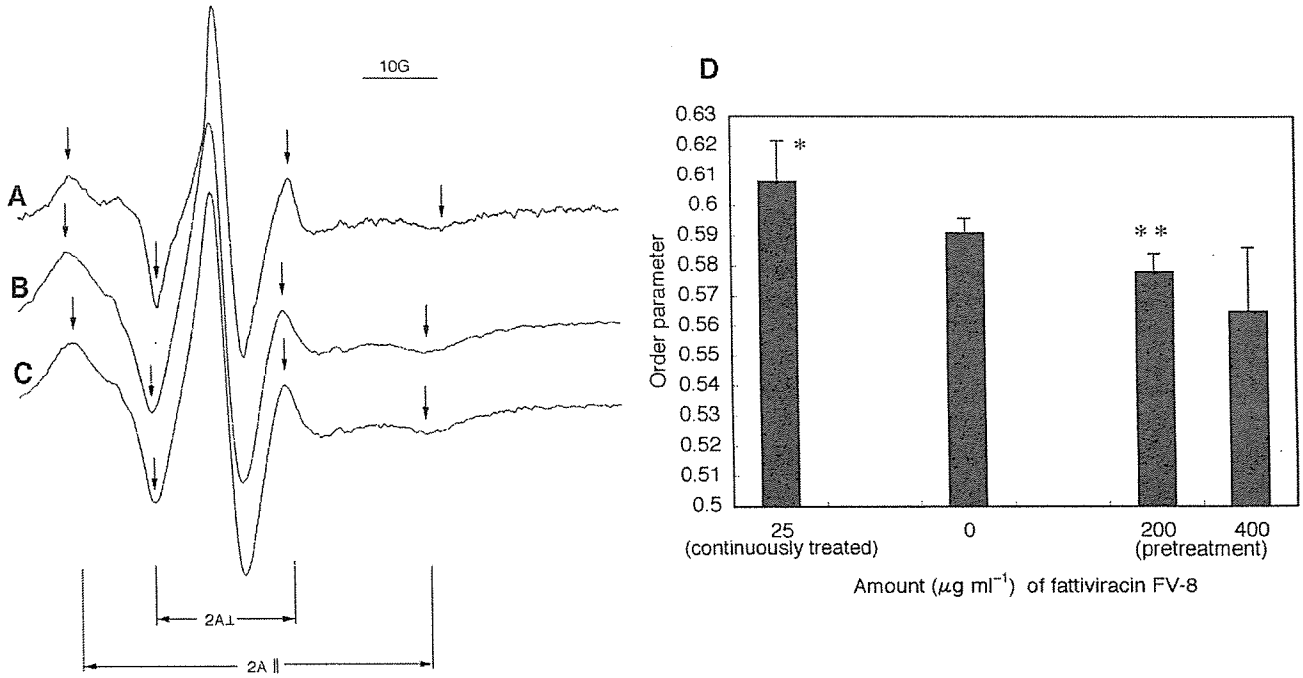

Fig. 3. Effects of fattiviracin FV-8 on the fluidity of the plasma membrane. ESR spectra of plasma membrane from MT-2 cells continuously treated with 25 μg ml^{-1} fattiviracin FV-8 (A), control MT-2 cells (B) and 200 μg ml^{-1} fattiviracin FV-8-pretreated MT-2 cells (C). The outer and inner hyperfine splitting, 2 $A_{//}$ and 2 $A_{\perp}$ were measured as shown by arrows. The scale of the horizontal axis (magnetic field) is shown as 10G. (D) MT-2 cells were treated with 25 μg ml^{-1} fattiviracin FV-8 and membrane fluidity was assessed in the presence of 25 μg ml^{-1} fattiviracin FV-8 (continuously treated, $n = 10$). MT-2 cells were pretreated with 200 and 400 μg ml^{-1} fattiviracin FV-8 and the fluidity was assessed in PBS (pretreatment, $n = 5$ each). Bars show the mean ± SD. *$P < 0.02$ compared with control (0 μg ml^{-1}) MT-2 cells ($n = 6$) and **$P < 0.01$ compared with control.

with 400 μg ml^{-1} fattiviracin FV-8, the glycolipid tended to enhance syncytium formation (Fig. S1C).

Effect of fattiviracin FV-8 on membrane fluidity

The electron spin resonance (ESR) spectra of MT-2 plasma membrane with 5-doxyl stearic acid (5-DSA) showed a typical pattern of anisotropic motion of the probe situated in the lipid bilayer (Fig. 3B). The ESR spectrum of MT-2 cells continuously treated with 25 μg ml^{-1} fattiviracin FV-8 showed a rather immobilized state (Fig. 3A), indicating that the motion of the 5-DSA spin probe was strongly restricted by the interaction with membrane constituents, probably incorporated fattiviracin FV-8 glycolipids. The order parameter was 0.608 ($n = 10$), significantly higher ($P < 0.02$) than that (0.591) of control MT-2 cells ($n = 6$) (Fig. 3D). When the cells were pretreated with 200 μg ml^{-1} fattiviracin FV-8, the ESR spectrum exhibited short $A_{//}$ (Fig. 3C) and the order parameter decreased to 0.578 ($n = 5$) (Fig. 3D), which was also significantly lower ($P < 0.01$) than the control MT-2 cells. When the cells were pretreated with 400 μg ml^{-1}, the order parameter tended to be lower than 200 μg ml^{-1}, but this was not significant due to undulation of the fluidity (Fig. 3D). Thus, fattiviracin FV-8 is a fluidity modulator, and the suppression and enhancement of membrane fluidity by the glycolipid were correlated with the decreased and increased susceptibility to HIV-1 infection and cell–cell fusion.

Theoretical mechanisms of antiviral activity and fluidity modulation by glycolipids

Both fattiviracin FV-8 and glycyrrhizin were fluidity modulators. Consequently, they showed similar effects on viral infection; first, the compounds were broad antiviral agents, especially against enveloped viruses; second, the compounds blocked cell–cell fusion induced by accumulation of cell-associated viral ligands and receptors; third, the compounds reduced the infectivity of virion itself when the viruses were pretreated; last, when cells were pretreated with high concentrations of the compounds, the cells exhibited enhanced susceptibility to viral infection and cell–cell fusion. All of the above effects can be explained by membrane fluidity modified by the compounds in terms of fusion-pore-formation due to accumulation of activated viral fusion peptides. A similar inhibitory effect of retrocyclin 2 on viral fusion and entry was reported, although retrocyclin 2 immobilized surface proteins by cross-linking membrane glycoproteins (Leikina

et al., 2005). Restricted movement of membrane molecules by cross-linking or decreased fluidity is actually critical to the entry of viruses, thus it can be applied to a new strategy to inhibit virus infection. As capsianoside G and fattiviracin FV-8 show similar potency (Table 1), both could be a potential candidate of broad antiviral agents.

Incorporation or exodus of movable macromolecules in or from the lipid-bilayer membrane produces dynamic changes in membrane fluidity, thus disturbing the lateral movement of proteins in the membrane. Amphipathic glycoproteins diffuse in and out the membrane through their hydrophilic and lipophilic domains. Diffusion efficiency may be determined by the amount of sugars, because longer sugar-chained molecules with more hydrophilic nature had less effect on HIV-1 infection (capsianoside G versus capsianoside A in Table 1). The presence of these molecules in the membrane may hamper the anisotropic movement of acyl chains of phospholipids. One can imagine that this 'diffusion and occupancy' may have a bearing on molecule movement in the membrane and in this manner influence viral entry, formation of synapses, and other membrane-mediated functions.

Experimental procedures

Cells and culture

MOLT-4, MOLT-4/HIV-1_{C-2} and MT-2 cells (Harada *et al.*, 1985) were cultured in RPMI1640 medium (Gibco BRL, Grand Island, NY) supplemented with 10% heat-inactivated fetal bovine serum (FBS), 2 mM L-glutamine, 100 IU ml^{-1} of penicillin and 0.1 mg ml^{-1} of streptomycin (complete medium). MAGI/CCR5 cells were cultured in Dulbecco minimal essential medium (ICN, Costa Mesa, CA) with 10% heat-inactivated FBS, 2 mM L-glutamine, 100 IU ml^{-1} penicillin, 0.1 mg ml^{-1} streptomycin, 0.1 mg ml^{-1} G418, 0.05 mg ml^{-1} hygromycin B and 0.05 mg ml^{-1} zeomycin as described (Song *et al.*, 2001).

Preparation of viruses

LAI (III_B) viruses (X4 HIV-1) were obtained from 3-day-old culture-supernatants of MOLT-4/HIV-1_{C-2} cells. JR-FL (R5 HIV-1) and 89.6 (X4R5 HIV-1) viruses were recovered by transfection of pJR-FL and p89.6, respectively, into COS-7 cells using Lipofectamine (Gibco) as described (Song *et al.*, 2001). The supernatants were filtered through 0.45 μm-pore-size filters and used as cell-free viruses.

Reagents

Sphingomyelin, sphingosine and lysophosphatidic acid were purchased from Sigma (St Louis, MO), dissolved at a concentration of 100 mg ml^{-1} in ethanol and stored at –20°C. The stock solution was diluted with phosphate-buffered saline (PBS) and sonicated for 10 min before use. Galactosylceramide (Galactocerebrosides from Sigma) and monosialoganglioside GM_1 (Sigma) were dissolved in ethanol at a concentration of 50 mg ml^{-1} and stored at –20°C. Capsianosides were extracted from *Capsicum annuum* and their structures were elucidated and reported elsewhere (Song *et al.*, 2001). Capsianosides were dissolved in methanol at 10 mg ml^{-1} and stored at –20°C until use. The volume of capsianosides required was dried in an eppendorf tube using a vacuum centrifugal concentrator, then dissolved in complete medium for each experiment. Fattiviracin FV-8 isolated from *Streptomycetes* was dissolved at a concentration of 50 mg ml^{-1} in PBS and stored at 4°C until use. 5-DSA was purchased from Sigma-Aldrich and stored at a concentration of 20 mg ml^{-1} in ethanol at 4°C. Anti-CD4 monoclonal antibody (mAb) Leu 3a and anti-CXCR4 mAb 12G5 were also purchased from Becton Dickinson (Lincoln Park, NJ) and R and D Systems (Minneapolis, MN) respectively.

Multinuclear activation of a galactosidase indicator assay

The MAGI/CCR5 cells (2×10^4 $well^{-1}$) that had been seeded the previous day on a flat 48 well plate were infected with LAI, JR-FL or 89.6 viruses. On day 2 post infection, infected MAGI/CCR5 cells were fixed with 1% formaldehyde and 2% glutaraldehyde in PBS for 5 min. Cells were then washed twice with PBS and incubated for 40 min at 37°C with staining solution (3 mM potassium ferrocyanide, 3 mM potassium ferricyanide, 1 mM $MgCl_2$ and 0.4 mg of Xgal in PBS). Blue nuclei were counted under a microscope (Kimpton and Emerman, 1992). Percentage infection was calculated as (% positive cells in test/% positive cells in control) × 100.

Adsorption of HIV-1

MAGI/CCR5 cells on a flat 48 well plate were incubated with 20 ng p24 of HIV-1 at 37°C for 1 h. The cells were washed twice with complete medium and lysed in 200 μl. The lysates were measured by p24 ELISA to assess the amount of adsorbed viruses. Percentage adsorption was calculated as (amount of p24 in test/amount of p24 in control) × 100.

Treatment of HIV-1 with fattiviracin FV-8

Viral supernatants were treated with serially diluted fattiviracin FV-8 at 37°C for 1 h and then ultracentrifuged at 100 000 *g* for 1 h at 4°C to obtain viral pellets. The pellets were resuspended with complete medium to remove the excess glycolipid and used to inoculate MAGI/CCR5 cells to assess infectivity. The resuspended viruses were also evaluated for the amount of p24 using ELISA.

Fusion assay

MOLT-4 and MOLT-4/HIV-1_{C-2} cells were used as target and effector cells, respectively, for the fusion assay. 0.5 ml (3×10^5) of MOLT-4 cells was mixed with the same amount of MOLT-4/HIV-1_{C-2} cells in the presence or absence of 20 μg ml^{-1} fattiviracin FV-8. In another experiment, MOLT-4 cells were treated with 400 μg ml^{-1} fattiviracin FV-8 at 37°C for 1 h and washed once

before mixing. The mixture (1 ml well^{-1}) was placed in a flat 24 well plate and cultured at 37°C for 24 h.

Measurement of membrane fluidity by ESR spectroscopy

One millilitre (7×10^6) of MT-2 cells was mixed with 1 ml of 60 μg ml^{-1} 5-DSA in PBS to give a final concentration of 30 μg ml^{-1}, and then incubated at 37°C for 20 min (Harada, 2005). The cells were washed 3 times with PBS to remove the free spin label. Pellets of cells were resuspended in 40 μl of PBS and drawn into a capillary tube, and the ends were sealed. The capillary tube was then placed into a quartz glass tube and taken from the P3 facility. Spectra were recorded at 37°C with a JES-RE1X ESR spectrometer (JEOL, Tokyo, Japan) equipped with a variable temperature control accessory. Instrument conditions were 2 min scan time, 5.0 mT sweep width, 0.1 mT field modulation width, 10 mW microwave power, and 0.3 s time constant. Figure 3 shows representative spectra, for which the outer hyperfine splitting indicates 2 $A_{//}$ and the inner one denotes 2 $A_{\perp}$: The horizontal axis reflects varying magnetic fields and the vertical axis represents absorption of microwaves. The order parameter (S) was calculated as follows; $S = (A_{//} - A_{\perp})/27.3G$.

P24 assay

The amount of HIV-1 core p24 was assessed by using HIV-1 p24 antigen ELISA (Cellular Products, Buffalo, NY) according to the manufacturer's protocol.

Statistical analysis

Statistical analyses were carried out using the Student's unpaired *t*-test, and a *P*-value of < 0.05 was statistically considered indicative of significance.

Acknowledgements

We thank W. Song and K. Nagao for their technical help and M. Uyeda and S. Yahara for supplying fattiviracin FV-8 and capsianosides respectively. The studies described in this manuscript were funded by the Ministry of Health, Labour and Welfare (Health Sciences Research Grants), and also supported in part by the Cooperative Research Project on Clinical and Epidemiological Studies of Emerging and Re-emerging Infectious Diseases (Renkei Jigyo: No. 78, Kumamoto University) of the Ministry of Education, Culture, Sports, Science, and Technology (Monbu-Kagakusho) of Japan.

References

Colman, P.M., and Lawrence, M.C. (2003) The structural biology of type I viral membrane fusion. *Nat Rev Mol Cell Biol* **4:** 309–319.

Gibbons, D.L., Erk, I., Reilly, B., Navaza, J., Kielian, M., Rey, F.A., and Lepault, J. (2003) Visualization of the target-membrane-inserted fusion protein of Semliki Forest virus by combined electron microscopy and crystallography. *Cell* **114:** 573–583.

Gibbons, D.L., Vaney, M., Roussel, A., Vigouroux, A., Reilly, B., Lepault, J., *et al.* (2004) Conformational change and protein–protein interactions of the fusion protein of Semliki Forest virus. *Nature* **427:** 320–325.

Habib, E.E., Yokomizo, K., Nagao, K., Harada, S., and Uyeda, M. (2001) Antiviral activity of fattiviracin FV-8 against human immunodeficiency virus type 1 (HIV-1). *Biosci Biotechnol Biochem* **65:** 683–685.

Harada, S. (2005) The broad anti-viral agent glycyrrhizin directly modulates the fluidity of plasma membrane and HIV-1 envelope. *Biochem J* **392:** 191–199.

Harada, S., Koyanagi, Y., and Yamamoto, N. (1985) Infection of HTLV-III/LAV in HTLV-I-carrying cells MT-2 and MT-4 and application in a plaque assay. *Science* **229:** 563–566.

Harada, S., Akaike, T., Yusa, K., and Maeda, Y. (2004a) Adsorption and infectivity of human immunodeficiency virus type 1 are modified by the fluidity of the plasma membrane for multiple-site binding. *Microbiol Immunol* **48:** 347–355.

Harada, S., Yusa, K., and Maeda, Y. (2004b) Heterogeneity of envelope molecules shown by different sensitivities to anti-V3 neutralizing antibody and CXCR4 antagonist regulates the formation of multiple-site binding of HIV-1. *Microbiol Immunol* **48:** 357–365.

Harada, S., Yusa, K., Monde, K., Akaike, T., and Maeda, Y. (2005) Influence of membrane fluidity on human immunodeficiency virus type 1 entry. *Biochem Biophys Res Commun* **329:** 480–486.

Kimpton, J., and Emerman, M. (1992) Detection of replication-competent and pseudotyped human immunodeficiency virus with a sensitive cell line on the basis of activation of an integrated β-galactosidase gene. *J Virol* **66:** 2232–2239.

Leikina, E., Delanoe-Ayari, H., Melikov, K., Cho, M., Chen, A., Waring, A.J., *et al.* (2005) Carbohydrate-binding molecules inhibit viral fusion and entry by crosslinking membrane glycoproteins. *Nat Immunol* **6:** 995–1001.

McDonald, D., Wu, L., Bohks, S.M., Kewal Ramani, V.N., Unutmaz, D., and Hope, T.J. (2003) Recruitment of HIV and its receptors to dendritic cell-T cell junctions. *Science* **300:** 1295–1297.

Modis, Y., Ogata, S., Clements, D., and Harrison, S.C. (2004) Structure of the dengue virus envelope protein after membrane fusion. *Nature* **427:** 313–319.

Plonsky, I., and Zimmerberg, J. (1996) The initial fusion pore induced by baculovirus gp64 is large and forms quickly. *J Cell Biol* **135:** 1831–1839.

Roche, S., and Gaudin, Y. (2002) Characterization of the equilibrium between the native and fusion-inactive conformation of rabies virus glycoprotein indicates that the fusion complex is made of several trimers. *Virology* **297:** 128–135.

Song, W., Yahara, S., Maeda, Y., Yusa, K., Tanaka, Y., and Harada, S. (2001) Enhanced infection of an X4 strain of HIV-1 due to capping and colocalization of CD4 and CXCR4 induced by capsianoside G, a diterpene glycoside. *Biochem Biophys Res Commun* **283:** 423–429.

Tsunakawa, M., Komiyama, N., Tenmyo, O., Tomita, K., Kawano, K., Kotake, C., *et al.* (1992a) New antiviral antibiotics, cycloviracins B_1 and B_2 I. Production, isolation, physico-chemical properties and biological activity. *J Antibiot* **45:** 1467–1471.

Tsunakawa, M., Kotake, C., Yamasaki, T., Moriyama, T., Konishi, M., and Oki, T. (1992b) New antiviral antibiotics, cycloviracins B_1 and B_2 I. Structure determination. *J Antibiot* **45:** 1472–1480.

Uyeda, M., Yokomizo, K., Miyamoto, Y., and Habib, E.E. (1998) Fattiviracin A1, a novel antiherpetic agent produced by streptomyces microflavus strain, 2445, I. Taxonomy, fermentation, isolation, physico-chemical properties and structure elucidation. *J Antibiot* **51:** 823–828.

Yokomizo, K., Miyamoto, Y., Nagao, K., Kumagae, E., Habib, E.E., Suzuki, K., *et al.* (1998) Fattiviracin A1, a novel antiherpetic agent produced by streptomyces microflavus strain, 2445, II. Biological properties. *J Antibiot* **51:** 1035–1039.

Supplementary material

The following supplementary material is available for this article online:

Fig. S1. Effects of fattiviracin FV-8 on cell–cell fusion. MOLT-4 cells were cocultured with MOLT-4/HIV-$1_{C\text{-}2}$ cells in the absence (A) or presence (B) of 20 μg ml^{-1} fattiviracin FV-8. MOLT-4 cells pretreated with 400 μg ml^{-1} fattiviracin FV-8 were cocultured with MOLT-4/HIV-$1_{C\text{-}2}$ cells (C). Bar, 100 μm.

This material is available as part of the online article from http://www.blackwell-synergy.com

Available online at www.sciencedirect.com
SCIENCE DIRECT®
Biochemical and Biophysical Research Communications 329 (2005) 480–486
BBRC
www.elsevier.com/locate/ybbrc

Influence of membrane fluidity on human immunodeficiency virus type 1 entry

Shinji Harada [a,*], Keisuke Yusa [a], Kazuaki Monde [a], Takaaki Akaike [b], Yosuke Maeda [a]

[a] *Department of Medical Virology, Graduate School of Medical Sciences, Kumamoto University, Kumamoto 860-8556, Japan*
[b] *Department of Microbiology, Graduate School of Medical Sciences, Kumamoto University, Kumamoto 860-8556, Japan*

Received 19 January 2005

Abstract

For penetration of human immunodeficiency virus type 1 (HIV-1), formation of fusion-pores might be required for accumulating critical numbers of fusion-activated gp41, followed by multiple-site binding of gp120 with receptors, with the help of fluidization of the plasma membrane and viral envelope. Correlation between HIV-1 infectivity and fluidity was observed by treatment of fluidity-modulators, indicating that infectivity was dependent on fluidity. A 5% decrease in fluidity suppressed the HIV-1 infectivity by 56%. Contrarily, a 5% increase in fluidity augmented the infectivity by 2.4-fold. An increased temperature of 40 °C or treatment of 0.2% xylocaine after viral adsorption at room temperature enhanced the infectivity by 2.6- and 1.5-fold, respectively. These were inhibited by anti-CXCR4 peptide, implying that multiple-site binding was accelerated at 40 °C or by xylocaine. Thus, fluidity of both the plasma membrane and viral envelope was required to form the fusion-pore and to complete the entry of HIV-1.

Keywords: HIV-1; Membrane fluidity; Receptor; Fusion; Multiple-site binding; Viral penetration

Human immunodeficiency virus type 1 (HIV-1) infects CD4-positive cells by a process of membrane fusion that is initiated by binding of the viral envelope glycoproteins, a trimeric complex of non-covalently associated gp120 and gp41 subunits, to two cell membrane components, CD4 and a coreceptor (CXCR4 or CCR5) belonging to the chemokine receptor family [1–3]. Previous reports have demonstrated that cell-to-cell fusion and/or HIV-1 cell to cell transfer requires recruitment of viral envelope proteins and HIV-1 receptors to the interface as a virological synapse [4,5]. It has also been proposed that an HIV-1 particle itself could use multiple-site binding of gp120 with receptors for completion of the infection [6–11]. The formation of functional fusion-pores must require the accumulation of a critical number of structurally changed gp41, six-helix bundles [12], induced by interaction with the coreceptor. The formation of ring-like assemblies of fusion proteins and cooperativity in the membrane-insertion process has been observed in studies of rabies [13], baculovirus [14], influenza virus [15], and Semliki Forest virus [16].

Since the lipid bilayer structure of the plasma membrane and the viral envelope is liquid or semi-ordered under physiological conditions, multiple-site attachment of a virion is thought to be achieved by recruitment of additional binding sites within the fluid mosaic membrane [17] due to fluidization of both the plasma membrane and viral envelope. Factors that modify the fluidization of the lipid bilayer are temperature, and amounts of lipids and cholesterol in the membrane [18]. Heating and cooling of infected cells during viral adsorption ostensibly increased and decreased the infectivity, respectively [11]. Changing the fluidization of the plasma membrane by detergent incorporation or antibody-binding also modified the level of HIV-1 infectivity [11]. Thus, we propose

* Corresponding author. Fax: +81 96 373 5132.
E-mail address: biodef@gpo.kumamoto-u.ac.jp (S. Harada).

0006-291X/$ - see front matter © 2005 Elsevier Inc. All rights reserved.
doi:10.1016/j.bbrc.2005.02.007

that HIV-1 induces a stable adhesion, due to mobility of receptors on the plasma membrane containing multiple gp120/receptor complexes (multiple-site binding), which facilitates the formation of a wide fusion-pore and efficient penetration of the virus into the target cell.

In order to gain more insight into the function of the membrane/envelope-fluidity in HIV-1 infection, we designed a series of experiments to examine the effects of fluidity-modulators on fluidization of the plasma membrane and HIV-1 envelope. We found that fluidity was logarithmically correlated with HIV-1 infectivity. These studies provide novel insights into the cell biology of retroviral penetration and demonstrate distinct roles for membrane fluidity at early stages of HIV-1 penetration.

Materials and methods

Cells and culture. MOLT-4, MOLT-4/HIV-$1_{C\text{-}2}$, MOLT-4/HIV-$1_{esc.C\text{-}2}$ [19], and MT-2 [20] cells were cultured in RPMI1640 medium (Gibco) supplemented with 10% heat-inactivated fetal bovine serum, 2 mM L-glutamine, 100 IU/ml penicillin, and 0.1 mg/ml streptomycin (complete medium). GHOST/CXCR4 cells were cultured in complete medium with 0.2 mg/ml G418, 0.05 mg/ml hygromycin B, and 2 mg/ml puromycin as described [21].

Preparation of viruses. Plaque-cloned HIV-$1_{C\text{-}2}$ viruses and their 0.5β-escaped HIV-$1_{esc.C\text{-}2}$ viruses [19,20] were obtained from 3-day-old culture-supernatants of MOLT-4/HIV-$1_{C\text{-}2}$ and MOLT-4/HIV-$1_{esc.C\text{-}2}$ cells, respectively. Human T-cell leukemia virus type I (HTLV-I)-transformed MT-2 cells were infected with C-2 viruses and cultured for 5 days. Progeny viruses in the supernatant were used as HIV-$1_{C\text{-}2(MT\text{-}2)}$. After filtration through a 0.45-μm pore-sized membrane, the supernatants were stored at −80 °C. X4 envelope-pseudotyped viruses with the luciferase reporter gene (NL43-luc pseudoviruses) were produced by the calcium phosphate transfection method [22]. The 293T cells were cotransfected with an envelope-deficient NL43 construct carrying the luciferase gene (pNL43-luc) and a pCXN2 vector expressing the envelope glycoprotein from pNL43.

Reagents. A CXCR4 antagonist T140 was provided by Fujii and co-workers [23]. The local anesthetic xylocaine (2%), which contains 20 mg/ml lidocaine and 0.0125 mg/ml epinephrine, was stored at room temperature (RT) and diluted with phosphate-buffered saline (PBS) or complete medium before use. D-α-Phosphatidylcholine dipalmitoyl (DPPC) was purchased from Sigma, dissolved at a concentration of 100 mg/ml in ethanol and was stored at 4 °C. The stock solution was diluted with PBS and sonicated for 10 min before use. There was no toxicity to cells observed at 0.2% xylocaine and 200 μg/ml DPPC. Five-doxyl stearic acid (5-DSA) was purchased from Aldrich and stored at a concentration of 20 mg/ml in ethanol at 4 °C.

CD45-depleted viral preparation. Fifty milliliters of culture supernatant containing viruses were mixed with 1 ml of anti-CD45 beads (Dynal Biotech ASA, Oslo, Norway), incubated at 37 °C for 40 min, and captured by a magnet held outside of the tube containing the sample [24]. The supernatant was removed and ultra-centrifuged to make a viral pellet, and fluidity was assessed with an untreated control.

Measurement of membrane fluidity in intact cells and viruses by electron spin resonance (ESR) spectroscopy. One milliliter (7×10^6) of cells or 50 ml of culture supernatant containing viruses (2–3 μg p24) were mixed with 1 ml of 60 μg/ml 5-DSA or 25 ml of 90 μg/ml 5-DSA in PBS, respectively, to make a final concentration of 30 μg/ml, and then incubated at 37 °C for 20 min. The cells were washed three times with PBS to remove the free spin label. The viruses were centrifuged at 114,000*g* for 1 h at 4 °C in a 60 Ti Beckman rotor. Pellets of cells or viruses were resuspended in 40 μl of PBS and drawn into a capillary tube, and the ends were sealed. The capillary tube was further placed into a quartz glass tube and taken from the P3 facility. Spectra were recorded with a JES-RE1X ESR spectrometer (JEOL, Tokyo, Japan) equipped with a variable temperature control accessory. Instrument conditions were 2 min scan time, 5.0 mT sweep width, 0.1 mT field modulation width, 10 mW microwave power, and 0.3 s time constant. Fig. 1 shows representative spectra, for which the outer hyperfine splitting indicates $2A_{\parallel}$, and the inner one denotes $2A_{\perp}$. The horizontal axis reflects varying magnetic fields and the vertical axis represents absorption of microwaves. The order parameter (S) was calculated as follows: $S = (A_{\parallel} - A_{\perp})/[A_{zz} - (A_{xx} + A_{yy})/2] = (A_{\parallel} - A_{\perp})/27.3$ G.

Membrane preparation. Cells (10^8) were resuspended in 2 ml buffer A solution [10 mM NaCl, 5 mM $MgCl_2$, 10 mM Tris–HCl (pH 7.4), and 0.02 mM phenylmethylsulfonyl fluoride (PMSF)], placed on ice for 15 min, and homogenized with 10 strokes of a tight-fitting Dounce homogenizer (Wheaton). The homogenate was diluted with 14 ml of cold buffer B [140 mM NaCl, 2 mM $MgCl_2$, 10 mM Tris–HCl (pH 7.4), and 0.4 mM PMSF]. After centrifugation at 1000*g* for 10 min, the supernatant was overlaid on a 32% sucrose solution and centrifuged at 180,000*g* for 1 h at 4 °C in a SW41 Ti Beckman rotor. The band in the interface was collected, pelleted, and resuspended in 500 μl of 0.1% Triton X-100 in PBS [25]. For viral envelope preparation, 50 ml of culture supernatant was centrifuged at 114,000*g* for 1 h at 4 °C. The viral pellet was resuspended in 2 ml of cold buffer A, placed on ice for 15 min, and sonicated for 10 min. Three milliliters of cold buffer B were then added, and applied to a sucrose gradient centrifugation. The collected sample was resuspended in 200 μl of 0.1% Triton X-100 in PBS.

Protein analysis. Protein concentrations in samples were determined by the BCA Protein assay kit (PIERCE, Rockford, IL). The cholesterol content was determined using an Amplex Red Cholesterol assay kit (Molecular Probes, Eugene, OR) according to the manufacturer's instructions. The amount of adsorbed HIV-1 was assessed by measuring the amount of viral core p24 using the HIV-1 p24 antigen ELISA (Cellular Products, Buffalo, NY) according to the manufacturer's protocol.

Blocking of the post-attachment enhancement (PAE) and infectivity assay with luciferase readout. GHOST/CXCR4 cells (2.5×10^4/well) that had been seeded the previous day on a flat 48-well plate were infected with 100 μl/well of NL43-luc pseudovirus. The viral adsorption took place at RT for 1 h. After washing once with complete medium, cells were incubated at 37 °C or 40 °C for 1 h in the presence or absence of T140 or and then washed once. Subsequently, the plate was incubated at 37 °C for 2 days, when the infected cells were lysed with 100 μl/well of luciferase assay buffer (Promega, Madison, WI). Luciferase activity was measured by adding 50 μl of the luciferase assay substrate (Promega) to 10 μl of cell lysate and then the light activity was read in a luminometer detector (Lumat LB 9501/16;EG and G Berthold, Bad Wilbad, Germany) [26].

Results and discussion

Measurement of fluidity of the intact plasma membrane and viral envelope

The dynamic conditions of the lipid-bilayer were studied by incorporating 5-doxyl stearic acid (5-DSA) spin probes into the plasma membrane and the viral envelope and recording electron spin resonance (ESR) spectra (Fig. 1). Plaque-cloned C-2 virus from X4 HIV-1_{LAI} and its neutralizing antibody (0.5β)-escaped virus, esc.C-2 virus [19,20], were used as viral preparations. The intact C-2 and esc.C-2 viruses were concentrated by ultra-centrifugation of culture-supernatants

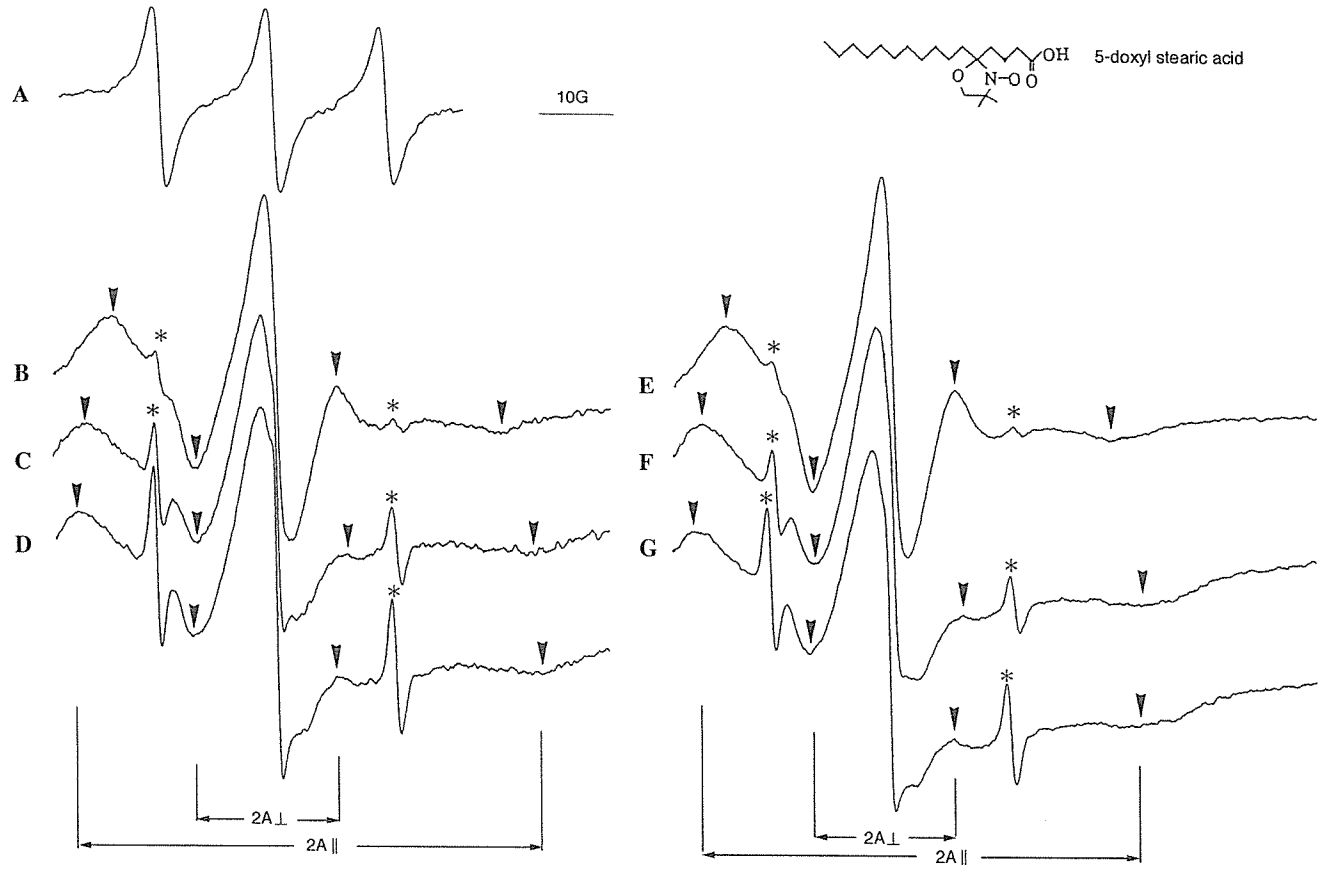

Fig. 1. ESR spectra of free 5-DSA (A), plasma membranes from intact MOLT-4/C-2 (B) and MT-2 (E) cells, and viral envelopes from intact C-2 (C), CD45-depleted C-2 (D), C-2(MT-2) (F), and CD45-depleted C-2(MT-2) (G) viruses. The outer and inner hyperfine splittings, $2A_{\parallel}$ and $2A_{\perp}$ were measured as shown by arrows. Asterisks show spectra of free 5-DSA remaining in each sample. Order parameters (S-values) of B, C, D, E, F, and G were calculated at 0.611, 0.729, 0.776, 0.585, 0.704, and 0.721, respectively. Scale of the horizontal axis (magnetic field) is shown as 10 G (gauss).

from C-2- and esc.C-2-chronically infected MOLT-4 cells (denoted as MOLT-4/C-2 and MOLT-4/esc.C-2 cells, respectively). MT-2 cells were infected with C-2 viruses. Resultant progeny viruses, C-2(MT-2) viruses, were also harvested and used for this study. To quantitate the membrane and envelope-fluidity, the order parameter (S-value) of each sample was calculated from the ESR spectra (Fig. 1) of 5-DSA-labeled cells or viruses at 37 °C (Table 1). The order parameter represents the flexibility of the probe.

Order parameters (0.685–0.738) of each 5-DSA-labeled virus were higher than those (0.582–0.598) of plasma membranes from which each virus was budded (Table 1). These elevated order parameters showed that the lipid-bilayer envelope of HIV-1 is highly ordered and rigid. According to cholesterol content in membrane preparations, cholesterol/protein (C/P) ratios of the viral envelope were higher than those of the plasma membrane from which the respective virus was derived, indicating that rigidity of the viral envelope could be due to high concentrations of cholesterol. The finding (Table 1) is in good agreement with the data reported by Aloia et al. [27,28]. These observations suggest that HIV-1 buds exclusively from the cholesterol-rich part or so-called "raft" of the plasma membrane [29,30].

Table 1
Order parameter and cholesterol/protein (C/P) of plasma membrane and viral envelope

Samples	Order parameter ($n = 3$)	Cholesterol/protein (μg/ml) [ratio] of plasma membrane or viral envelope
Group I		
MOLT-4/C-2 cell	0.598 ± 0.009	48/210 [0.229]
HIV-1_{C-2}	0.738 ± 0.012	40/145 [0.276]
CD45-depleted C-2	0.752 ± 0.017	NT[a]
Group II		
MOLT-4/esc.C-2 cell	0.585 ± 0.003	40/140 [0.286]
HIV-$1_{esc.C-2}$	0.690 ± 0.019	55/185 [0.351]
CD45-depleted esc.C-2	0.763 ± 0.013	NT
Group III		
MT-2 cell	0.582 ± 0.007	20/160 [0.125]
HIV-$1_{C-2(MT-2)}$	0.685 ± 0.032	70/215 [0.326]
CD45-depleted C-2(MT-2)	0.708 ± 0.011	NT

[a] NT, not tested.

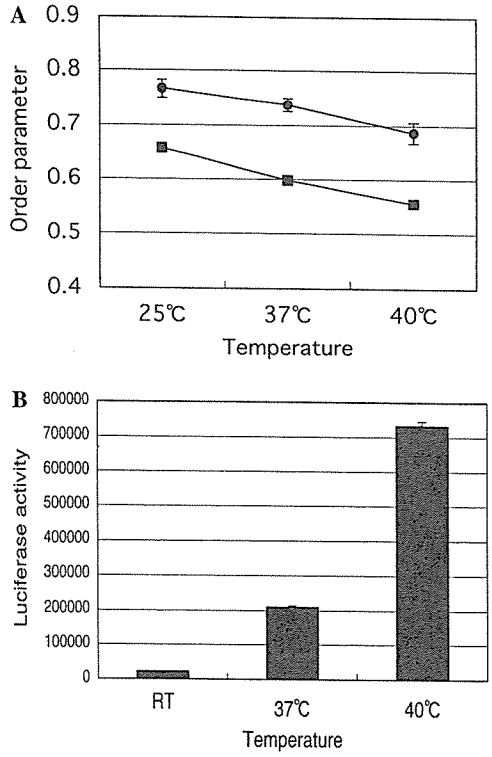

Fig. 2. Dependence of the fluidity (A) of the plasma membrane from intact MOLT-4/C-2 cells (square) and the viral envelope from intact C-2 viruses (circle) on temperature, and dependence of HIV-1 infectivity (B) on temperature. GHOST/CXCR4 cells in a flat-bottomed 48-well plate were treated with 100 μl/well of NL43-luc virus at room temperature (RT), 37 and 40 °C for 1 h. After washing once with complete medium, the infected cells were cultured at 37 °C for 2 days before measuring luciferase activity. All experiments in (A,B) were carried out in triplicate, and solid lines and bars show the means ± SD.

HIV-1 preparations by ultra-centrifugation were reported to contain a substantial amount of microvesicles on which CD45, a leukocyte integral membrane protein, is found [24]. A CD45-based immunoaffinity depletion for removing CD45-positive microvesicles from viral preparations increased the order parameter of each viral preparation (Table 1), indicating that fluidity of the viral envelope from crude preparations was underestimated, and thus the viral envelope was further ordered. An increase in temperature from 25 to 40 °C decreased order parameters of 5-DSA-labeled C-2 viruses and labeled MOLT-4/C-2 cells (Fig. 2A). Dependency of the order parameters on temperature and cholesterol-concentrations indicates that the ESR method using 5-DSA quantitatively measured the fluidity of both the plasma membrane and viral envelope from the probe-labeled intact cells and virions, respectively.

Correlation of membrane fluidity and HIV-1 infectivity

GHOST/CXCR4 cells incubated with X4 envelope-pseudotyped viruses with the luciferase reporter gene (NL43-luc pseudovirus) at room temperature (RT), 37 and 40 °C for 1 h showed luciferase activities of 22026, 209035, and 731975, respectively, which were inversely correlated with the order parameters (Figs. 2A and B). We have previously shown that GHOST/CXCR4 cells increased HIV-1 infectivity by 1.4-fold but decreased order parameters (increased membrane fluidity) by 0.97-fold upon treatment with 0.05% Tween 20 [11]. In addition, anti-HLA-II-bound MT-2 cells decreased the level of HIV-1 infectivity by 0.38-fold but increased the parameter (or decreased the fluidity) by 1.03-fold [11]. In order to further confirm that the membrane fluidity is responsible for HIV-1 infectivity, in this study, GHOST/CXCR4 cells were treated with serial doses of xylocaine or D-α-phosphatidylcholine dipalmitoyl (DPPC), which are fluidity-modulators [31]. Addition of increased doses of xylocaine during viral adsorption at 37 °C for 1 h increased NL43-luc infectivity dose-dependently up to 2.5-fold (Fig. 3A). When MT-2 cells were incubated with C-2 virus in the presence of 0.2% xylocaine for 1 h, increased infectivity of 1.7-fold was also observed. Membrane fluidity of 0.2% xylocaine-treated MT-2 cells was increased by 4.2%, calculated by the decreased order parameter (Fig. 3C). For an unknown reason, treatment of GHOST/CXCR4 cells with DPPC fluctuated in the response of viral infectivity depending on the dose (Fig. 3B). High doses (200 μg/ml) of DPPC increased the infectivity by 32%, but 10 μg/ml DPPC decreased it by 25% (Fig. 3B). We observed a similar fluctuation of infectivity with repeated experiments. Depending on the fluctuation of infectivity, 200 μg/ml DPPC decreased order parameters by 1.7% and 10 μg/ml increased them by 2.3% (Fig. 3C). The expression of CD4 and CXCR4 in MT-2 cells was unchanged with treatment of 0.2% xylocaine or 10 μg/ml DPPC (data not shown). When all the above data were plotted on a semi-logarithmic scale, an inverse correlation between infectivity ratio and order parameter ratio was obtained (Fig. 4). A 5% increase in the order parameter decreased HIV-1 infectivity by 56%, whereas a 5% decrease in the order parameter induced a 2.4-fold increase in infectivity. Thus, a small change in membrane fluidity could be indispensable to modifying HIV-1 infectivity.

The dynamic structure or mobility of lipid-bilayered membranes consists of anisotropic rotation of the phospholipid acyl chain, flip-flop and lateral diffusion of phospholipids or other molecules [18]. The order parameter of 5-DSA-labeled membranes preferentially represents the anisotropic motion of the long molecular axis of the spin-labeled probes, and thus inversely indicates the flexibility of the incorporated probe. Spin-labeled derivatives of stearic acid have been widely employed to investigate the lipid-bilayer properties of either intact cells or purified membrane preparations. In this study, manipulating the fluidization of both the

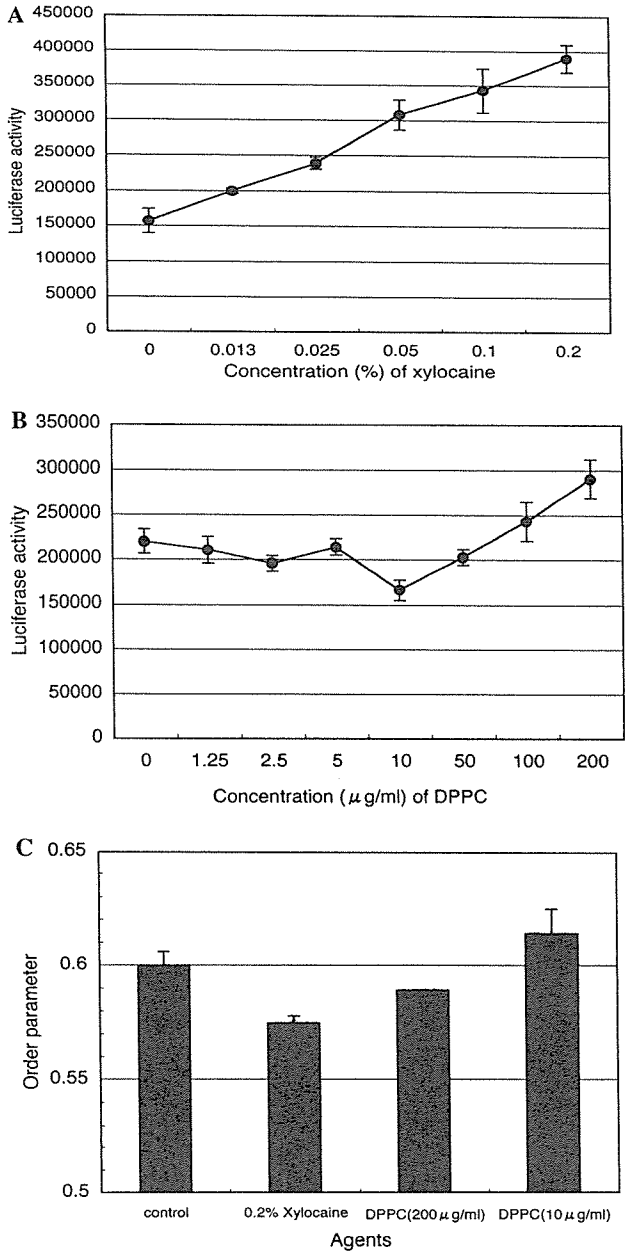

Fig. 3. Effects of xylocaine (A) and DPPC (B) on HIV-1 infectivity and fluidity of plasma membranes from MT-2 cells (C). (A,B) GHOST/CXCR4 cells in a flat-bottomed 48-well plate were treated with a 100 μl/well mixture of NL43-luc virus with serially diluted xylocaine or DPPC at 37 °C for 1 h. After washing once with complete medium, the cells were cultured at 37 °C for 2 days before assessing luciferase activity. (C) MT-2 cells (7×10^6) were treated with 0.2% xylocaine or DPPC (10 or 200 μg/ml) at 37 °C for 30 min, washed once and resuspended with 1 ml of complete medium. The cells were then labeled with 5-DSA and examined by ESR spectroscopy. All experiments in (A–C) were carried out in triplicate, and solid lines and bars show the means ± SD.

plasma membrane and viral envelope logarithmically affected the HIV-1 infectivity (Fig. 4). Thus, analyses of membrane fluidity of intact cells and intact viruses may provide a unique virological approach.

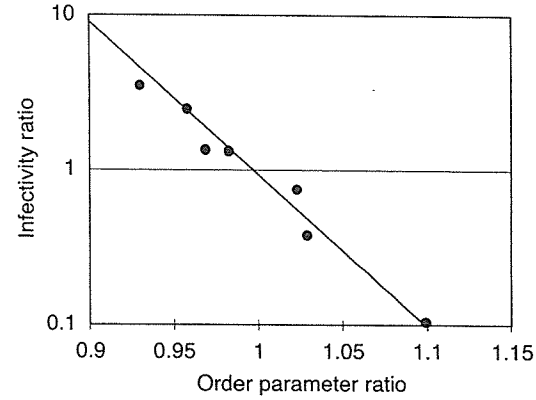

Fig. 4. Relationship between HIV-1 infectivity and membrane fluidity. The infectivity ratio was calculated as follows: luciferase activity in test/luciferase activity in control, and the order parameter ratio as: order parameter in test/order parameter in control. Circles from the left indicate 40 °C, 0.2% xylocaine, 0.05% Tween 20, 200 μg/ml DPPC, 10 μg/ml DPPC, anti-HLA-II and 25 °C.

Inhibition of post-attachment enhancement of HIV-1 by anti-CXCR4 peptide T140

Increasing the temperature from RT to 40 °C for 1 h of the post-adsorption phase increased infectivity by 2.6-fold of control in (Fig. 5A). This phenomenon is hereafter referred to as post-attachment enhancement (PAE). The same PAE by 1.5-fold was observed when the virus-attached cells were treated with 0.2% xylocaine at 37 °C for 1 h (Fig. 5B). Thus, PAE was closely associated with increased fluidity of both the plasma membrane and viral envelope (Figs. 2A and 3C). In order to confirm that the PAE was the result of multiple-site binding of an HIV-1 virion, the effects of anti-CXCR4 peptide T140 on PAE were examined. When GHOST/CXCR4 cells were treated with T140 before being infected with NL43-luc pseudovirus, 1 μM T140 inhibited 95% of infection. After the viral adsorption at RT for 1 h, the post-adsorption step was carried out at either 37 or 40 °C (Fig. 5A) in the presence or absence of 1 μM T140. Increasing the temperature to 40 °C during the post-adsorption step augmented the level of infection by 2.6 times. PAEs from RT to both 37 and 40 °C were strongly abrogated by 1 μM T140 (Fig. 5A). The PAE induced by 0.2% xylocaine was also abolished by 1 μM T140 (Fig. 5B). This indicated that T140 could restrain viruses from forming further multiple-site binding by occupying CXCR4.

Engagement of the gp120/160 trimer with co-receptors induces gp41 rearrangement and exposure of the hydrophobic amino acid fusion domain, leading to fusion. The triggered fusion-activated gp41 structures are rod-like with a bundle of six helices [12]. It is conceivable that HIV-1 penetration into the cell requires a fusion-pore wide enough for the viral core to pass through. Accumulation of substantial numbers of fusion-acti-

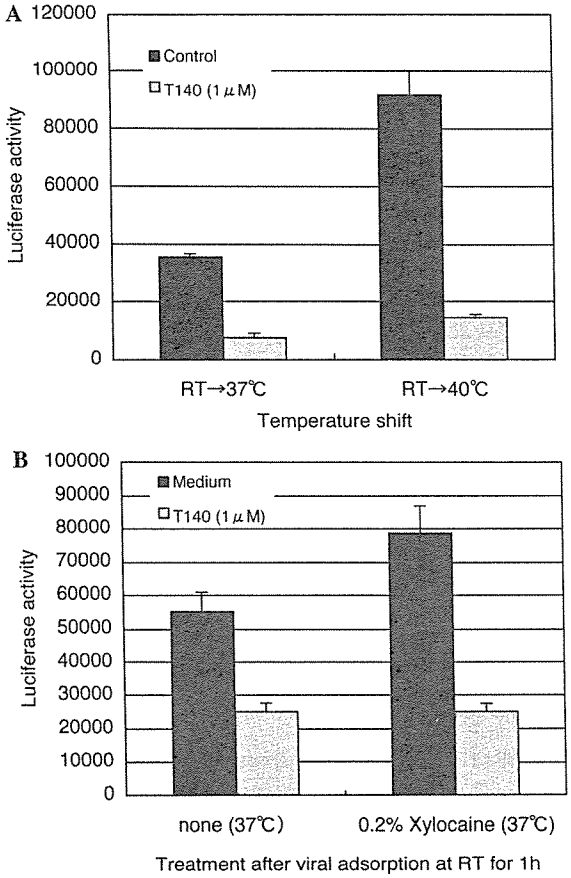

Fig. 5. Effects of T140 on post-attachment enhancement (PAE) at 40 °C (A) or by 0.2% xylocaine (B). GHOST/CXCR4 cells that had been seeded the previous day on a flat 48-well plate were infected with 100 μl/well of NL43-luc pseudovirus. The viral adsorption took place at room temperature (RT) for 1 h. After washing once with complete medium, cells were incubated at 37 or 40 °C (A), or with or without 0.2% xylocaine (B), for 1 h in the presence or absence of T140 and then washed once. The plate was incubated at 37 °C for 2 days and luciferase activity was measured. All experiments in (A,B) were carried out in triplicate, and solid lines and bars show the means ± SD.

vated gp41 structures must be necessary for this purpose. Cell–cell fusion is temperature-dependent [32], and it has been reported that there is a time lag of 10–20 min between the six-helix bundle formation and the fusion after transfer from 31.5 to 37 °C. This indicates that the formation of fusion-pores requires the critical number of six-helix bundles [33]. We have also reported that PAE at 40 °C required a time lag of 20–30 min to be recognized for blocking the enhancement by T140 after transfer from RT to 40 °C [11]. This suggests that PAE also requires the accumulation of gp120/receptor complexes just as cell–cell fusion requires it [33]. All enhancements observed as PAE due to temperature shifts (RT to 37 and 40 °C) and 0.2% xylocaine-treatment were strongly inhibited by T140 (Figs. 5A and B), indicating that multiple-site binding was functioning and was accelerated by fluidization.

Suppressing the fluidity of the plasma membrane and/or viral envelope could be one of new anti-HIV strategies to overcome varieties of HIV-1 because fluidity plays an important role in the infectivity due to the formation of multiple-site binding and fusion-pore. Further studies will be needed to clarify the relation between modifying the membrane fluidity and viral entry.

Acknowledgments

The studies described in this manuscript were funded by the Ministry of Education, Culture, Sports, Science and Technology, and the Ministry of Health, Labour and Welfare (Health Sciences Research Grants), Japan.

References

[1] E.A. Berger, HIV entry and tropism: the chemokine receptor connection, AIDS 11 (Suppl. A) (1997) S3–S16.
[2] T.L. Hoffman, R.W. Doms, Chemokines and coreceptors in HIV/SIV-host interactions, AIDS 12 (Suppl. A) (1998) S17–S26.
[3] T. Dragic, An overview of the determinants of CCR5 and CXCR4 co-receptor function, J. Gen. Virol. 82 (2001) 1807–1814.
[4] D. McDonald, L. Wu, S.M. Bohks, V.N. KewalRamani, D. Unutmaz, T.J. Hope, Recruitment of HIV and its receptors to dendritic cell–T cell junctions, Science 300 (2003) 1295–1297.
[5] C. Jolly, K. Kashefi, M. Hollinshead, Q. Sattentau, HIV-1 cell-to-cell transfer across an env-induced, actin-dependent synapse, J. Exp. Med. 199 (2004) 283–293.
[6] S.P. Layne, M.J. Merges, M. Dembo, J.L. Spouge, P.L. Nara, HIV requires multiple gp120 molecules for CD4-mediated infection, Nature 346 (1990) 277–279.
[7] L. Picard, G. Simmons, C.A. Power, A. Meyer, R.A. Weiss, P.R. Clapham, Multiple extracellular domains of CCR-5 contribute to human immunodeficiency virus type 1 entry and fusion, J. Virol. 71 (1997) 5003–5011.
[8] E.J. Platt, K. Wehrly, S.E. Kuhmann, B. Chesebro, D. Kabat, Effects of CCR5 and CD4 cell surface concentrations on infections by macrophagetropic isolates of human immunodeficiency virus type 1, J. Virol. 72 (1998) 2855–2864.
[9] S. Manes, G. del Real, R.A. Lacalle, P. Lucas, C. Gomez-Mouton, S. Sanchez-Palomino, R. Delgado, J. Alcami, E. Mira, C. Martinez-A, Membrane raft microdomains mediate lateral assemblies required for HIV-1 infection, EMBO Rep. 1 (2000) 190–196.
[10] S. Harada, K. Yusa, Y. Maeda, Heterogeneity of envelope molecules shown by different sensitivities to anti-V3 neutralizing antibody and CXCR4 antagonist regulates the formation of multiple-site binding of HIV-1, Microbiol. Immunol. 48 (2004) 357–365.
[11] S. Harada, T. Akaike, K. Yusa, Y. Maeda, Adsorption and infectivity of human immunodeficiency virus type 1 are modified by the fluidity of the plasma membrane for multiple-site binding, Microbiol. Immunol. 48 (2004) 347–355.
[12] P.R. Clapham, A. McKnight, Cell surface receptors, virus entry and tropism of primate lentiviruses, J. Gen. Virol. 83 (2002) 1809–1829.
[13] S. Roche, Y. Gaudin, Characterization of the equilibrium between the native and fusion-inactive conformation of rabies virus glycoprotein indicates that the fusion complex is made of several trimers, Virology 297 (2002) 128–135.